Persistent gating deficit and increased sensitivity to NMDA receptor antagonism after puberty in a new mouse model of the human 22q11.2 micro-deletion syndrome – a study in male mice

Journal:	*Journal of Psychiatry and Neuroscience*
Manuscript ID	JPN-15-0381.R1
Manuscript Type:	Research
Date Submitted by the Author:	n/a
Complete List of Authors:	Didriksen, Michael; H. Lundbeck A/S, Synaptic transmission Fejgin, Kim; H. Lundbeck A/S, Synaptic transmission Nilsson, Simon; University of Cambridge, Cambridge, Behavioural and Clinical Neuroscience Institute Birknow, Michelle; H. Lundbeck A/S, Synaptic Transmission Grayton, Hannah; Eli Lilly, Lilly Centre for Cognitive Neuroscience Larsen, Peter; H. Lundbeck A/S, Synaptic transmission Lauridsen, Jes; H. Lundbeck A/S, Synaptic transmission Nielsen, Vibeke; H. Lundbeck A/S, Synaptic transmission CELADA, PAU; Institut d\'Investigacions Biomèdiques August Pi i Sunyer (IDIBAPS), IDIBAPS; Institut d\'Investigacions Biomèdiques de Barcelona (IIBB-CSIC), Neurochemistry and Neuropharmacology Santana, Noemi; Centro de Investigación Biomédica en Red de Salud Mental, CIBERSAM Kallunki, Pekka; H. Lundbeck A/S, Neurodegeneration Christensen, Kenneth; H. Lundbeck A/S, Neurodegeneration Werge, Thomas; Copenhagen University Hospital Roskilde, Research Institute of Bilogcal Psychiatry Stensbøl, Tine; H. Lundbeck A/S, Synaptic transmission Egebjerg, Jan; H. Lundbeck A/S, Neurodegeneration Gastambide, Francois; Eli Lilly, Lilly Centre for Cognitive Neuroscience Artigas, Francesc; Institut d'Investigacions Biomèdiques de Barcelona (IIBB), Centro de Investigación Biomédica en Red de Salud Mental (CIBERSAM), Consejo Superior de Investigaciones Científicas (CSIC), Neurochemistry and Neuropharmacology Bastlund, Jesper; H. Lundbeck A/S, Synaptic transmission Nielsen, Jacob; H. Lundbeck A/S, Synaptic transmission
Keywords:	Animal models < Neuroscience, Psychiatric genetics < Neuroscience, Electrophysiology < Neuroscience, Antipsychotics < Neuroscience, Neuropsychiatry < Neuroscience

Persistent gating deficit and increased sensitivity to NMDA receptor antagonism after puberty in a new mouse model of the human 22q11.2 micro-deletion syndrome – a study in male mice

Michael Didriksen, PhD[1]; Kim Fejgin, PhD[1]; Simon RO Nilsson PhD[2,3]; Michelle R Birknow, MSc[1];Hannah M Grayton, PhD[4]; Peter H Larsen PhD[1]; Jes B Lauridsen, PhD[1]; Vibeke Nielsen, BSc[1]; Pau Celada, PhD[5]; Noemi Santana, PhD[6]; Pekka Kallunki, PhD[1]; Kenneth V Christensen PhD[1]; Thomas M Werge, PhD[7]; Tine B Stensbøl, PhD[1]; Jan Egebjerg, PhD[1]; Francois Gastambide, PhD[4]; Francesc Artigas, PhD[5,6]; Jesper F Bastlund, PhD[1]; Jacob Nielsen, PhD[1]

[1]H. Lundbeck A/S, Research DK, Ottiliavej 9, Valby 2500, Denmark.[2]Department of Psychology, University of Cambridge, Cambridge, CB2 3EB, UK. [3]Behavioural and Clinical Neuroscience Institute, University of Cambridge, Cambridge, CB2 3EB, UK. [4]Lilly Centre for Cognitive Neuroscience, Lilly Research Laboratories, Eli Lilly & Co. Ltd, Erl Wood Manor, Sunninghill Road, Windlesham, GU20 6PH, UK. [5]Institut d'Investigacions Biomèdiques de Barcelona, CSIC-IDIBAPS, Barcelona, Spain. [6]Centro de Investigación Biomédica en Red de Salud Mental (CIBERSAM), Spain. [7]Institute of Biological Psychiatry, MHC Sct. Hans, Copenhagen Mental Health Services; Institute of Clinical Sciences, Faculty of Medicine and Health Sciences, University of Copenhagen; iPSYCH - The Lundbeck Foundation's

Initiative for Integrative Psychiatric Research, Boserupvej,

DK-4000 Roskilde, Denmark

Word counts – Abstract: 249. Intro, Materials, Results, and Discussion: 3844

4 figures + 2 tables

57 references

Corresponding Author:

Michael Didriksen M.Sc. Ph.D

H. Lundbeck A/S

Ottiliavej 9

2500 Valby

Denmark

Tel: +45 36 43 31 11

Fax +45 36 43 82 58

Email: mdi@lundbeck.com

Abstract

Background: The hemizygous 22q11.2 micro-deletion is a common copy number variant in humans. The deletion confers high risk of neurodevelopmental disorders including autism and schizophrenia. Up to 41% of deletion carriers experience psychotic symptoms. Methods: We present a new mouse model (Df(h22q11)/+) of the deletion syndrome (22q11.2DS) and report on the most comprehensive study undertaken in 22q11.2DS models. The study was conducted in male mice. Results: We found elevated post-pubertal NMDA receptor antagonist induced hyper-locomotion, age-independent prepulse inhibition (PPI) deficits and increased acoustic startle response (ASR). The PPI deficit and increased ASR was resistant to antipsychotic treatment. The PPI deficit was not a consequence of impaired hearing measured by auditory brain stem responses. The Df(h22q11)/+ mice also displayed increased amplitude of loudness-dependent auditory evoked potentials. Prefrontal cortex and dorsal striatal (DStr) elevations of the dopamine metabolite DOPAC and increased DStr expression of the AMPA receptor subunit GluR1 was found. The Df(h22q11)/+ mice did not deviate from wild-type mice in a wide range of other behavioural and biochemical assays. Limitations: The 22q11.2 micro-deletion has incomplete penetrance in humans and the severity of disease depends on the complete genetic makeup in

concert with environmental factors. In order to obtain more marked phenotypes reflecting the severe conditions related to 22q11.2DS it is suggested to expose the Df(h22q11)/+ mice to environmental stressors which may unmask latent psychopathology. Conclusion: The Df(h22q11)/+ model will be a valuable tool for increasing our understanding of the aetiology of schizophrenia and other psychiatric disorders associated with the 22q11DS.

Introduction

The 22q11.2 hemizygous micro-deletion confers very high risk of neurodevelopmental disorders including autism and schizophrenia (22q11.2 deletion syndrome - 22q11.2DS). The estimated prevalence is approximately 1:2000 (1). The International Consortium on Brain and Behavior in 22q11.2 has recently reported the cumulated prevalence of schizophrenia to be 24% in adolescence and 41% in adulthood (2). Studies of schizophrenia patients find that 22q11.2 deletion account for approximately 0.3% of the cases (3).

Despite massive efforts there is still no coherent understanding of the aetiology of schizophrenia - a highly heritable heterogeneous disorder with strong environmental influence (4;5). Several neurotransmitters are implicated in the disorder: Glutamate (6), GABA- (7), dopamine- (DA) (8), and acetylcholine- signaling (9) have all been implicated in the disease aetiology and manifestation. The cognitive impairment and negative symptomatology have been related to dysfunction in regulation of glutamate-GABA transmission leading to excitatory-inhibitory imbalances (7). Like in schizophrenia(10;11), cognition (12) and information processing is disrupted in children with 22q11.2 deletion, who have not (yet) developed schizophrenia (13;14). Due to the highly increased risk of developing schizophrenia and the phenotypic overlap between schizophrenia and the 22q11.2DS,

studies of the consequence of the 22q11.2 deletion provides a unique opportunity to add to the understanding of the aetiology of schizophrenia and other related psychiatric disorders, which eventually may lead to novel drugs targeting the core of the disease.

Five transgenic mouse models of the 22q11.2DS have been generated by different research groups (Table 1). These models have recently been reviewed by Hiroi et al. that also provide an overview of key genes in the 22q11 region (15). Inconsistent results are reported from assays addressing schizophrenia-relevant cognitive functions (Unpublished observations) whereas studies of other symptom domains are more consistent (see Table 1). Decreased prepulse inhibition (PPI) and increased acoustic startle response (ASR) is consistently observed (LgDel (16), Df1/+ (17) and Df(16)A$^{+/-}$) (18). However, hearing was recently shown to be impaired in the Df1/+ mouse (19), raising the possibility that hearing loss rather than altered sensorimotor gating might underlie PPI deficits in 22q11DS mouse models.

The LgDel (16), Df1/+ (17) and Df(16)A+/- (18) mice used in the referred studies are non-congenic. Genetic background (20) and environmental factors (21) may influence phenotypic expression. To be able to control for these factors and to ensure sufficient access to mice we have generated a new congenic mouse model (Df(h22q11)/+) of the 22q11.2DS as part of a large multi-site collaboration. Here we report on an

extensive characterisation of these mice using a set of assays related to the pathophysiology of schizophrenia. We find that the Df(h22q11)/+ mice display phenotypes relevant for modelling aspects of schizophrenia-related symptoms including increased post-pubertal NMDA antagonist sensitivity and age-independent PPI and ASR deficits. We show that these impairments were not a result of impaired hearing. The Df(h22q11)/+ mice also displayed increased amplitude of loudness dependent auditory evoked potentials (LDAEP), prefrontal cortex (PFC) and dorsal striatal (DStr) elevations of the DA metabolite DOPAC, and increased DStr expression of the AMPA receptor subunit GluR1. The Df(h22q11)/+ mice did not deviate from wild-type (WT) mice in a range of other behavioural and biochemical assays.

Materials and methods

See Supplement for details.

Animals

The Df(h22q11)/+ mouse line was generated by TaconicArtemis (Köln, Germany). Animals were bred by mating WT C57BL/6N females with hemizygotic Df(h22q11)/+ males to avoid any placental or maternal care effects of the deletion. Animals were weaned at 3 weeks and tail biopsies were collected for PCR based genotyping. Mice were group-housed (2 WT mice and 2 hemizygotes from the same litter per cage) under

controlled laboratory conditions (12:12 hr light-dark cycle; 20±2°C; 30-70% humidity) in standard mouse cages with sawdust bedding, environmental enrichment (plastic house and paper for nesting), and food and water available ad libitum. Post-surgery mice were single housed (see appendix – loudness dependence auditory evoked potentials. All experiments were carried out using littermate controls. The experiments used 27 cohorts (N=12-95) of male mice aged 6-26 weeks (Figure A2). The selection of cohorts and animals for individual experiments was not randomized. All studies were carried out in accordance with the local legislation according to the European Union regulation (directive 2010/63 of 22 September 2010) and UK Animals (Scientific Procedures) Act 1986. The studies were approved by the Barcelona School of Medicine Institutional Animal Care and Use Committee or the Danish National Committee for Ethics in Animal Experimentation.

Drugs

Clozapine (obtained from Novartis) was dissolved in 0.1 M hydrochloride and diluted with saline. Gabazine (SR95531, obtained from Sigma-Aldrich, St Louis, MO) was dissolved in 0.2 M NaCl. Haloperidol (obtained from Sigma) was dissolved in 0.1 M tartaric acid and diluted with saline. Phencyclidine (PCP), hydrochloride (synthesised by Lundbeck) was dissolved in 0.1 M methanesulfonic acid and diluted with saline. (S)-(+)-ketamine (obtained from Sigma-Aldrich) was

dissolved in 5% (w/v) glucose solution at a concentration of 10 mg/ml.

For the microdialysis studies veratridine and PCP were purchased from Sigma-Aldrich (Madrid, Spain) and nomifensine from Tocris (Madrid, Spain). Veratridine was dissolved in DMSO (5 mM) and nomifensine (1 mM) in artificial cerebrospinal fluid (aCSF).

Basal characterisation. Animals were characterised in the hot plate, rotarod, beam-walk, bright open-field, locomotor activity, and elevated plus maze.

Prepulse Inhibition (PPI) of the acoustic startle response (ASR). The procedure is extensively described elsewhere (22). Six cohorts of animals were tested without drug treatment (age: 6-21 weeks). Two cohorts were treated with either clozapine (s.c. 10 ml/kg; 13-weeks old) or haloperidol (s.c. 10 ml/kg; 15-weeks old).

NMDAr antagonist induced hyperactivity. Following a 60 min habituation phase to a novel environment, Df(h22q11)/+ and WT littermates were treated with PCP or S(+)-ketamine (s.c. 10 ml/kg) and their activity was monitored for a further 60 min.

Anatomy. Gross characterisation including assessment of brain weight, ventricular size, hippocampal structure,

myelination, cortical thickness and layer composition using cortical NeuN and parvalbumin immunoreactivity and solochrome staining was conducted.

Western analyses. A targeted screen (Peggy–Simple Western analyses) was carried out for proteins in the PFC, DStr and hippocampus. Markers showing significant changes across genotypes were replicated twice. The first replication used new dilutions from each of the 11 samples per genotype separately, while the second replication used 1 pooled sample for each genotype, which was run twice.

Tissue content measured by HPLC. PFC and DStr tissue content of DA, dihydroxyphenylacetic acid (DOPAC), Homovanillic acid (HVA), noradrenaline (NA), 5-hydroxytryptamine (5-HT) and 5-Hydroxyindoleacetic acid (5-HIAA) was collected and analysed as previously described (23).

Microdialysis in freely-moving animals. The functional state of DStr DA-transmission was assessed as previously described (24). Briefly, after collection of baseline DA dialysate fractions, extracellular DA levels were measured following reverse dialysis by application of the depolarizing agent veratridine (50 µM) (local 20 min pulse), and the dopamine/noradrenaline transporter uptake inhibitor nomifensine (50 µM) (local application during eight

fractions). PCP (2.5 + 2.5 mg/kg, s.c.) was administered systemically the following day to the same animals. Microdialysis measures were taken at AP +0.5, ML −1.7, DV −4.5 from Bregma (25).

Electrophysiology

Loudness dependent auditory evoked potentials (LDAEPs). Auditory stimuli (white noise, 5 ms duration with 1 ms rise and fall) were presented to awake freely moving mice at different intensity levels (60, 70, 80, 90 and 100 dB) with a 6 s inter-stimulus interval. 20 min EEG recordings were made during auditory stimulation. Grand average auditory evoked potentials from the auditory cortex (AuC) were constructed consisting of a 100 ms pre-stimulus baseline and a 900 ms post-stimulus interval. The peak N1- and P2-amplitudes were determined as the most negative deflection 10-25 ms post-stimulus and the most positive deflection 22-65 ms post-stimulus, respectively. Peak-to-peak N1/P2-amplitudes were determined at each intensity. Linear regression between peak-to-peak N1/P2 amplitude and sound intensity was calculated and the LDAEP was determined as the mean slope of the linear regression.

Auditory induced brainstem response (ABR). ABRs were recorded with auditory stimulation to the left and right ears

of anaesthetised animals with hollow ear bars guiding sound waves to the external auditory meatus. Three subdermal electrodes were inserted; the active electrode was placed at the vertex, the reference electrode was placed at the ear being tested, and the ground electrode was placed near the opposite ear. ABRs were recorded during a series of click stimuli (duration: 50 µsec, rate: 20 Hz/s, intensity: 30-100 dB in 5-dB steps) with 500 repeats per intensity level. Stimuli were presented to one ear, with the non-stimulated ear being blocked with an earplug. At each intensity ABRs were averaged and analysed within a 7 ms post-stimulus window. ABR thresholds were identified by visual inspection blinded to the genotype for both left and right ears and defined as the lowest intensity evoking a deflection of the ABR wave. The ABR protocol used was modified from Fuchs et al. (2013).

Low-frequency cortical oscillation (LFO). Medial prefrontal cortical (mPFC) LFO power was assessed at baseline and following systemic PCP treatment (10 mg/kg, s.c.) as previously described (26). Recordings were made at AP: + 2.1, ML: -0.2 to -0.4, DV: -1 to -2.5 mm from Bregma (25).

mPFC $GABA_A$ receptor function. mPFC $GABA_A$ receptor ($GABA_AR$) function was assessed by examining discharge rates of putative pyramidal neurons in control conditions and during local application of the $GABA_AR$ antagonist gabazine as previously

described (27). Recordings were made at AP: + 2.1, L: -0.2 to -0.4, DV: -1 to -2.5 mm from Bregma (25).

Statistics

Statistical analysis was performed by SigmaPlot (v11.2, Systat Software Inc.) or SPSS (v21.0, IBM Corp). Data were analysed by either 2-way analysis of variance (ANOVA), 2-way repeated measure (RM) ANOVA, or by t-test. Post-hoc test was conducted by the Holm-Sidak method. For the t-test Mann-Whitney Rank Sum Test was used if normality (Shapiro-Wilk) or equal variance (Levene) test failed.

No adjustments were made for multiple testing beyond the post-hoc tests. Data were visually inspected for outliers. No obvious outliers were identified and all data were included in the analysis. We only had few missing values. The missing values were handled by SigmaPlot using a general linear model.

Results

See Table 1 and Table A1 for summary of results.

Generation of mice and basic phenotyping

The Df(h22q11)/+ mouse line was generated by deletion of the human 22q11.2DS orthologous genomic region on mouse chromosome 16 (Figure 1a; Figure A1). Expression levels of deleted genes in cortical areas were examined by microarray analysis (Figure 1b). Except for Tssk1, Vpreb2, and Cdc45

expression of all detected genes in the deleted region were significantly reduced to roughly 50% of the expression in WT mice. Absolute expression levels assessed by RNAseq analysis of cortex in WT mice showed that Tssk1, Vpreb2, and Cdc45 along with the undetected Tssk2 and Gsc2 genes were very lowly expressed suggesting that the apparent unchanged expression of these genes are due to very low signal-to-noise ratio in the microarray detection (data not shown). Expression of the flanking gene Car15 was also reduced by 50% in the Df(h22q11)/+ mouse, while expressions of other flanking genes were unaltered. Only around 40% of newborn pups were hemizygous indicating reduced conception or intrauterine survival (Df(h22q11)/+ fraction ≈ 0.40, p = 0.042) (Figure A3). In the following studies, hemizygous males were compared to WT male littermates.

Overall, Df(22q11.2)/+ mice appeared healthy with grossly normal behaviour including pain sensitivity (hotplate: 50-56°C), motor function (beam-walking, locomotor activity, rotarod) and anxiety response (bright open field, elevated plus maze) (Figure A3) and with normal brain weight and gross morphology (cortical layer composition, hippocampal structures, parvalbumin positive interneuron counts and myelin patterns) (Figure A3 and A4).

Behaviour

Pre-pulse inhibition (PPI). PPI was significantly reduced in Df(h22q11)/+ mice (Fig 2a). Data were collapsed across prepulse intensities as there was no genotype × prepulse intensity (5, 10, 15dB) interaction. The PPI impairment was stable during development and consistently observed in 6 independent cohorts of 6-21 weeks old animals. The impairment was resistant to treatment with haloperidol (Figure 2b) and clozapine (Figure 2c) representing typical and atypical antipsychotics, respectively. Clozapine impaired PPI in the WT mice at the highest dose tested (2 mg/kg).

Acoustic startle response (ASR). Df(h22q11)/+ mice had increased ASR. The increased ASR was observed in 6 independent cohorts of 6-21 weeks old animals (Figure 2d). Haloperidol did not attenuate the increased ASR (Figure 2e). Clozapine decreased ASR in both WT and Df(h22q11)/+ mice. However, not genotype × treatment interaction effect was observed (Figure 2f).

PCP-induced hyperactivity. Df(h22q11)/+ mice showed hyper-reactivity to PCP induced locomotor activity in an age-dependent manner. The hyper-reactivity was seen in 9-week old but not 7-week old mice (Figure 2g).

S-(+)-ketamine-induced hyperactivity. Df(h22q11)/+ mice at 26 weeks of age showed hyper-reactivity to ketamine induced locomotor activity (Figure 2h).

Biochemistry

Tissue content. Df(h22q11)/+ mice had increased levels of DOPAC in the PFC (Figure 3a) and DStr (Figure 3b) whereas the levels of DA, HVA, NA, 5-HT, and 5-HIAA were unaffected.

Microdialysis in freely-moving animals. Df(h22q11)/+ and WT mice did not differ in baseline DStr DA, DOPAC, HVA, and glutamate levels (Figure 3c). Local administration of the sodium channel opener veratridine (Figure 3d) and the dopamine/noradrenaline reuptake inhibitor nomifensine (Figure 3e) increased DA equally in Df(h22q11)/+ and WT mice. Similarly, PCP increased DStr DA equally in Df(h22q11)/+ and WT mice following both the first and second PCP challenge (Figure 3f).

Western analyses. Df(h22q11)/+ showed decreased PFC NeuN and increased DStr GluR1 levels (Figure 3g). In a replication study using pooled samples from WT and Df(h22q11)/+ mice, respectively, the DStr GluR1 increase was confirmed while the PFC NeuN signal failed to replicate. There were no effects of genotype on levels of the 14 additional markers measured (Table 2).

Electrophysiology

Auditory induced brainstem response (ABR) threshold. Df(h22q11)/+ and WT mice did not differ in ABR threshold (Figure 4a). The ABR threshold did not exceed the previously defined hearing deficit criterion (55 dB SPL) (19).

Loudness dependent auditory evoked potentials (LDAEP). The Df(h22q11)/+ mice showed increased LDAEPs in AuC (Figure 4d-e). There was significant increase in P1/N1 and N1/P2 amplitudes. The Df(h22q11)/+ mice showed increased LDAEP at higher sound intensities, the N1/P2 amplitudes were increased at 90 dB ($p < 0.001$) and 100 dB ($p < 0.001$). Similar results were generated for other cortical brain regions, with differences in N1 amplitude as the main contributing component (data not shown). There was no effect of genotype on latency at any sound intensity (data not shown).

mPFC low frequency oscillations. There was no difference between Df(h22q11)/+ and WT mice on baseline or PCP-induced attenuation of cortical LFOs (Figure 4b). PCP decreased cortical LFOs.

mPFC $GABA_AR$ function. There was no difference between Df(h22q11)/+ and WT mice on baseline or $GABA_AR$ antagonist induced elevation of pyramidal neuron spike frequency (Figure

4c).

Discussion

In this paper we report on the generation and characterisation of a new 22q11DS mouse model with focus on assays relevant for the pathophysiology of schizophrenia. The Df(h22q11)/+ mice had age-independent and antipsychotic-resistant gating deficits measured by PPI. They had increased acoustic startle response and increased amplitude of loudness-dependent auditory evoked potentials. Also, the Df(h22q11)/+ mice exhibited increased NMDAr antagonist-induced locomotion, but in contrast to PPI, this effects was only observed post puberty. The 22q11.2 deletion resulted in increased DStr and PFC DOPAC levels as would be expected by the deletion of the COMT gene. Among other markers explored (figure 3 and table 2) we saw a reduction of DStr GluR1 expression.

PPI deficits and ASR changes have previously been reported in other 22q11DS mouse models (16-18). We confirmed these findings in our model and further examined the age dependency, response to antipsychotic treatment and possible hearing confounds. We found that the PPI and ASR changes in Df(h22q11)/+ mice are robust (observed in 6 independent cohorts), present before puberty, and persisting across ages. This effect mirrors the reduced PPI found in human 22q11.2 deletion carriers, which precede onset of puberty and

potential development of schizophrenia symptoms (13;14). Chronic middle ear infection and elevated click-response ABR threshold have been observed in the Df1/+ mouse model (19) raising the possibility that hearing loss at low intensities rather than sensorimotor gating deficits *per se* underlie the PPI deficits found in the 22q11DS mouse models. We addressed this by measuring ABR thresholds and found those to be unchanged in the Df(h22q11)/+ mice. This, together with the increased amplitude of auditory evoked potentials found in the LDAEP assay indicate that hearing is not reduced in the Df(h22q11)/+ mouse. Thus, the decrease in sensorimotor gating observed in the Df(h22q11)/+ mouse is not caused by hearing loss. The contrasting ABR findings between the Df(h22q11)/+ and Df1/+ mouse model (19) may be due to differences in strain or environmental conditions affecting the risk of ear infection.

The PPI and ASR impairments were resistant to antipsychotic treatment (haloperidol and clozapine), which is in overall agreement with the effect of these drugs in the clinical setting. In schizophrenia patients, classical antipsychotics working through D2/D3 receptor blockade reduce the psychotic symptoms without affecting PPI deficits (28;29). The findings for the new generation of antipsychotics with multi-receptor profiles are more mixed (28;30;31) and a cross-sectional study by Kumari (32) provided indirect evidence for clozapine being superior to haloperidol on PPI deficits in

schizophrenia patients, which is not reflected by the present data from the Df(h22q11)/+ mice.

Similar to the Df1/+ mouse (33), we found that Df(h22q11)/+ mice displayed increased locomotor activity in response to the NMDAr antagonists PCP and Ketamine. Interestingly, we further found that the effect was age-dependent and only observed after puberty (9- but not 7-week old animals). As schizophrenia is characterised by onset of overt symptoms during or after puberty (34) and glutamatergic dysfunctions (35;36), our data suggest that the Df(h22q11)/+ mouse may model aberrant NMDAr-related neurodevelopment trajectories associated with the disorder. The pre-pubertal and age-independent PPI deficits found in the Df(h22q11)/+ mice suggest that these sensorimotor gating deficits are due to biological perturbation other than what drives the NMDAr antagonist phenotype.

Biochemical assays revealed that the Df(h22q11)/+ mice had elevated PFC and DStr tissue content of the DA metabolite DOPAC. This phenotype may be explained by the haploinsufficiency for COMT, which catalyses the demethylation of DA. The role of COMT is well established in low-DAT density brain regions such as the PFC (37;38) whereas there are contrasting findings in striatum (39;40). The present data also support a role of COMT in striatal DA function. Despite the reduced expression of COMT and consequent increase in DOPAC we saw no changes in tissue content of DA and HVA, NA or

5-HT. The Df(h22q11)/+ mice also showed normal DStr DA release following PCP administration and local application of veratridine or nomifensine. DA release is involved in, but temporally dissociated from, NMDA antagonist-induced locomotor activity (41). The observed hypersensitivity to NMDAr blockade is likely not caused by hypersensitivity of the DA system in the Df(h22q11)/+ mice as release of DA is unchanged. This is further supported by the lack of locomotor hyper-responsivity to amphetamine in these mice (unpublished data). GluR1 was the only glutamatergic related marker (GluR2, NR2A, or NR2B, VGluT1) explored showing differential expression and we did not observe any changes in GABA related markers ($GABA_A$ α1, KCC2, VGAT, GAD 65/67). Furthermore, PFC GABAergic-glutamatergic interaction measured as $GABA_AR$ antagonism induced pyramidal cell discharge rates was not affected, and measures of PCP-induced attenuation of low frequency cortical oscillations showed preserved function of cortical neuronal networks in the Df(h22q11)/+ mice. Thus, expression of most receptors for the major transmitters is not altered and the mechanism responsible for increased behavioural responsivity to NMDAr blockade is unknown, which should be investigated further in future studies.

In line with the increased ASR, the amplitude of auditory evoked potentials were increased in Df(h22q11)/+ mice. The amplitude of auditory evoked potentials is decreased in schizophrenia (42) whereas mixed results have been found for

LDAEP. In some studies LDAEP have been found to be reduced in schizophrenia patients but these studies were not designed to account for difference in symptomatology (43;44). In a recent study by Wyss et al. (45) increased LDAEP was found in schizophrenia patients with predominant negative symptoms, which interestingly is also prominent in the symptomatology of patients with the 22q11.2DS (46-48) together with increased auditory event related potentials (49). Negative symptoms is also prominent in autism another disorder associated with the 22q11.2DS and increased amplitude of auditory evoked potentials have been reported in autism related syndromes like fragile X (50) and in animal models of autism (51;52). We have not assessed behavioural functions related to negative symptomatology in the present paper. However, reports of a reduced progressive ratio response in Df(16)A+/- mice (53) supports negative symptom-like behaviour in these mice (54). Hence the Df(h22q11)/+ mouse may also prove to be a useful model for aspects of the negative symptomatology in psychiatric disorders.

Limitations

Genetic mouse models provide insight into the consequence of the mutation in a specific genetic and environmental context. More marked changes might have been anticipated from introducing a high risk genetic variant comprising more than 25 genes into the mouse. However, it is important to keep in

mind that the 22q11.2 micro-deletion has incomplete penetrance in humans, expression and severity of disease depends on the complete genetic makeup (20) in concert with environmental influences. Thus, the Df(h22q11)/+ mouse is more appropriately thought of as a liability model rather than a disease model. This is in line with our previous findings that CNVs conferring high risk of mental disorders significantly affect structure and function of the brain in healthy human carriers (55). In order to obtain more marked phenotypes reflecting the severe conditions related to 22q11.2DS it is suggested to combine the Df(h22q11)/+ mouse with environmental stressors as used by Giovanoli et al. (56), which may unmask latent psychopathology. Giovanoli and colleagues showed how unpredictable stress during puberty resulted in PPI deficits and increased sensitivity to amphetamine and MK-801 in mice exposed to prenatal immune activation. In contrast, Harper et al showed how reduced social interaction in Sept5 KO mice, one of the 22q11.2 genes, could be rescued by reducing the level of stress (21), clearly demonstrating interaction between genotype and environment.

Sex differences in the behaviour of children with 22q11.2DS have been reported (57). Thus, it is highly relevant to explore sex differences in the mouse. In the present paper only male mice were included. Pilot studies conducted in our lab comparing male and female Df(h22q11)/+ mice did not reveal differences in motor function, seizure threshold, anxiety, or

amphetamine-induced locomotion. The studies have to be repeated and extended before firm conclusions can be made.

We did only observe few changes in protein expression. Additional synaptic fractionation might increase the resolution of the analysis, particularly with respect to synaptic proteins. However, the method used allowed us to investigate both synaptic (e.g. PSD95) and astrocytic markers (e.g. GFAP).

Conclusion

Here we show how the Df(h22q11)/+ mouse model reflects different developmental aspects of the 22q11.2DS and schizophrenia including changes in information processing and NMDAr antagonist responsiveness. Furthermore, the present findings extends previous reports on other 22q11.2DS mouse models by showing age-independent and antipsychotic-resistant gating deficits that are not confounded by reduced hearing. This model will be a valuable tool for further understanding the aetiology of schizophrenia and other psychiatric disorders with the ultimate goal of developing novel and improved drugs.

Funding and Disclosure

MD is an employee and shareholder of H. Lundbeck A/S. KF is an employee of H. Lundbeck A/S. SRON is an employee of University of Cambridge, UK. MRB is an employee of H. Lundbeck A/S. HM Grayton is an employee of Eli Lilly & Co. Ltd, UK. PHL is an employee of H. Lundbeck A/S. JBL is an employee of H. Lundbeck A/S. VN is an employee and shareholder of H. Lundbeck A/S. PC is an employee of IDIBAPS, Spain. NS is an employee of CIBERSAM, Spain. PK is an employee and shareholder of H. Lundbeck A/S. KVC is an employee and shareholder of H. Lundbeck A/S. TMW is an employee of Copenhagen Mental Health Services, Denmark. TMW received consultant and lecture fees from H. Lundbeck A/S. TBS is an employee and shareholder of H. Lundbeck A/S. JE is an employee and shareholder of H. Lundbeck A/S. FG is an employee of Eli Lilly & Co. Ltd, UK. FA is an employee of CSIC, Spain. FA received consultant fees from Lundbeck A/S and is member of the scientific advisory board of Neurolixis. He is also co-inventor of patents on RNAi technologies in collaboration with nLife Therapeutics. JFB is an employee and shareholder of H. Lundbeck A/S. JN is an employee of H. Lundbeck A/S.

Acknowledgements

The research leading to these results was conducted as part of NEWMEDS and received support from the Innovative Medicine Initiative Joint Undertaking under grant agreement n° 115008 of which resources are composed of EFPIA in-kind contribution and financial contribution from the European Union's Seventh Framework Programme (FP7/2007-2013). This work was further supported by grants from the Danish Advanced Technology Foundation (File no. 001-2009-2) and by the Instituto de Salud Carlos III, Centro de Investigación Biomédica en Red de Salud Mental (CIBERSAM).

We thank Annette Bjørn, Dorte Clausen, Kasper Larsen, Kirsten Jørgensen, Leticia Campa, Mercedes Nuñez, Noemi Jurado, Pia M. Carstensen, and Susanne Herskind-Hansen for skilful technical assistance.

Reference List

1. Shprintzen RJ. Velo-cardio-facial syndrome: 30 Years of study. Dev.Disabil.Res Rev 2008;14(1):3-10.

2. Schneider M, Debbane M, Bassett AS, Chow EWC, Fung WLA, Van den Bree M, Owen M, Murphy KC, Niarchou M, Kates WR, et al. Psychiatric disorders from childhood to adulthood in 22q11.2 deletion syndrome: results from the International Consortium on Brain and Behavior in 22q11.2 Deletion Syndrome. Am J Psychiatry 2014 Jun 1;171(6):627-39.

3. Rees E, Walters JT, Chambert KD, O'Dushlaine C, Szatkiewicz J, Richards AL, Georgieva L, Mahoney-Davies G, Legge SE, Moran JL, et al. CNV analysis in a large schizophrenia sample implicates deletions at 16p12.1 and SLC1A1 and duplications at 1p36.33 and CGNL1. Hum Mol Genet 2014 Mar 15;23(6):1669-76.

4. Harrison PJ, Weinberger DR. Schizophrenia genes within cortical neural circuits. Mol-Psychiatry 2005 Jan;10(1):5.

5. Ripke S, Neale BM, Corvin A, Walters JTR, Farh KH, Holmans PA, Lee P, Bulik-Sullivan B, Collier DA, Huang H, et al. Biological insights from 108 schizophrenia-

associated genetic loci. Nature 2014 Jul 22;511(7510):421-7.

6. Javitt DC, Zukin SR. Recent advances in the phencyclidine model of schizophrenia. Am J Psychiatry 1991 Oct;148(10):1301-8.

7. Pocklington AJ, Rees E, Walters JT, Han J, Kavanagh DH, Chambert KD, Holmans P, Moran JL, McCarroll SA, Kirov G, et al. Novel Findings from CNVs Implicate Inhibitory and Excitatory Signaling Complexes in Schizophrenia. Neuron 2015 Jun 3;86(5):1203-14.

8. Laruelle M, Abi-Dargham A, van Dyck CH, Gil R, D'Souza CD, Erdos J, McCance E, Rosenblatt W, Fingado C, Zoghbi SS, et al. Single photon emission computerized tomography imaging of amphetamine-induced dopamine release in drug-free schizophrenic subjects. Proc.Natl.Acad.Sci.USA 1996 Aug 20;93(17):9235-40.

9. Raedler TJ, Bymaster FP, Tandon R, Copolov D, Dean B. Towards a muscarinic hypothesis of schizophrenia. Mol Psychiatry 2007 Mar;12(3):232-46.

10. Elvevag B, Goldberg TE. Cognitive impairment in schizophrenia is the core of the disorder. Crit Rev Neurobiol 2000;14(1):1-21.

11. Braff D, Stone C, Callaway E, Geyer M, Glick I, Bali L. Prestimulus effects on human startle reflex in normals and schizophrenics. Psychophysiology 1978 Jul 1;15(4):339-43.

12. Hooper SR, Curtiss K, Schoch K, Keshavan MS, Allen A, Shashi V. A longitudinal examination of the psychoeducational, neurocognitive, and psychiatric functioning in children with 22q11.2 deletion syndrome. Res Dev.Disabil. 2013 May;34(5):1758-69.

13. Sobin C, Kiley-Brabeck K, Karayiorgou M. Associations between prepulse inhibition and executive visual attention in children with the 22q11 deletion syndrome. Mol Psychiat 2004 Nov 2;10(6):553-62.

14. Sobin C, Kiley-Brabeck K, Karayiorgou M. Lower prepulse inhibition in children with the 22q11 deletion syndrome. Am J Psychiatry 2005 Jun 1;162(6):1090-9.

15. Hiroi N, Takahashi T, Hishimoto A, Izumi T, Boku S, Hiramoto T. Copy number variation at 22q11.2: from rare variants to common mechanisms of developmental neuropsychiatric disorders. Mol Psychiatry 2013 Nov;18(11).

16. Long JM, LaPorte P, Merscher S, Funke B, Saint-Jore B, Puech A, Kucherlapati R, Morrow BE, Skoultchi AI,

Wynshaw-Boris A. Behavior of mice with mutations in the conserved region deleted in velocardiofacial/DiGeorge syndrome. Neurogenetics 2006 Aug 10;7(4):247-57.

17. Paylor R, McIlwain KL, McAninch R, Nellis A, Yuva-Paylor LA, Baldini A, Lindsay EA. Mice deleted for the DiGeorge/velocardiofacial syndrome region show abnormal sensorimotor gating and learning and memory impairments. Hum Mol Genet 2001 Nov 1;10(23):2645-50.

18. Stark KL, Xu B, Bagchi A, Lai WS, Liu H, Hsu R, Wan X, Pavlidis P, Mills AA, Karayiorgou M, et al. Altered brain microRNA biogenesis contributes to phenotypic deficits in a 22q11-deletion mouse model. Nat Genet 2008 May 11;40(6):751-60.

19. Fuchs JC, Zinnamon FA, Taylor RR, Ivins S, Scambler PJ, Forge A, Tucker AS, Linden JF. Hearing loss in a mouse model of 22q11. 2 deletion syndrome. PLoS ONE 2013 Jan 1;8(11):e80104.

20. Suzuki G, Harper KM, Hiramoto T, Sawamura T, Lee M, Kang G, Tanigaki K, Buell M, Geyer MA, Trimble WS, et al. Sept5 deficiency exerts pleiotropic influence on affective behaviors and cognitive functions in mice. Hum Mol Genet 2009 May 1;18(9):1652-60.

21. Harper KM, Hiramoto T, Tanigaki K, Kang G, Suzuki G, Trimble W, Hiroi N. Alterations of social interaction through genetic and environmental manipulation of the 22q11.2 gene Sept5 in the mouse brain. Hum Mol Genet 2012 Aug 1;21(15):3489-99.

22. Fejgin K, Nielsen J, Birknow MR, Bastlund JF, Nielsen V, Lauridsen JB, Stefansson H, Steinberg S, Sorensen HBD, Mortensen TE, et al. A mouse model that recapitulates cardinal features of the 15q13.3 microdeletion syndrome including schizophrenia- and epilepsy-related alterations. Biol Psychiat 2014 Jul 14;76(2):128-37.

23. Adell A, Sarna GS, Hutson PH, Curzon G. An in vivo dialysis and behavioural study of the release of 5-HT by p-chloroamphetamine in reserpine-treated rats. Brit J Pharmacol 1989 Apr 30;97(1):206-12.

24. Masana M, Bortolozzi Aa, Artigas F. Selective enhancement of mesocortical dopaminergic transmission by noradrenergic drugs: therapeutic opportunities in schizophrenia. Int J Neuropsychopharmacol 2011 Feb 1;14(1):53-68.

25. Paxinos G, Franklin KBJ. The Mouse Brain in Stereotaxic Coordinates. London: Elsevier Academic Press; 2008.242 p.

26. Kargieman L, Santana N, Mengod G, Celada P, Artigas F. Antipsychotic drugs reverse the disruption in prefrontal cortex function produced by NMDA receptor blockade with phencyclidine. Proc.Natl.Acad.Sci.U.S.A 2007 Sep 11;104(37):14843-8.

27. Lladó-Pelfort L, Santana N, Ghisi V, Artigas F, Celada P. 5-HT1A receptor agonists enhance pyramidal cell firing in prefrontal cortex through a preferential action on GABA interneurons. Cereb Cortex 2012 Jul 1;22(7):1487-97.

28. Mackeprang T, Kristiansen KT, Glenthoj BY. Effects of antipsychotics on prepulse inhibition of the startle response in drug-naive schizophrenic patients. Biol.Psychiatry 2002 Nov 1;52(9):863-73.

29. During S, Glenthoj BY, Andersen GS, Oranje B. Effects of dopamine D2/D3 blockade on human sensory and sensorimotor gating in initially antipsychotic-naive, first-episode schizophrenia patients. Neuropsychopharmacol. 2014 Dec;39(13):3000-8.

30. Duncan E, Szilagyi S, Schwartz M, Kunzova A, Negi S, Efferen T, Peselow E, Chakravorty S, Stephanides M, Harmon J, et al. Prepulse inhibition of acoustic startle in subjects with schizophrenia treated with olanzapine or haloperidol. Psychiatry Res. 2003 Aug 30;120(1):1-12.

31. Aggernaes B, Glenthoj BY, Ebdrup BH, Rasmussen H, Lublin H, Oranje B. Sensorimotor gating and habituation in antipsychotic-naive, first-episode schizophrenia patients before and after 6 months' treatment with quetiapine. Int.J.Neuropsychopharmacol. 2010 Nov;13(10):1383-95.

32. Kumari V, Soni W, Sharma T. Normalization of information processing deficits in schizophrenia with clozapine. Am.J.Psychiatry 1999 Jul;156(7):1046-51.

33. Kimoto S, Muraki K, Toritsuka M, Mugikura S, Kajiwara K, Kishimoto T, Illingworth EL, Tanigaki K. Selective overexpression of Comt in prefrontal cortex rescues schizophrenia-like phenotypes in a mouse model of 22q11 deletion syndrome. Transl Psychiatry 2012 Aug 1;2(8):e146-16.

34. Castle D, Sham P, Murray R. Differences in distribution of ages of onset in males and females with schizophrenia. Schizophrn Res 1998 Oct 8;33(3):179-83.

35. Olney JW, Farber NB. Glutamate receptor dysfunction and schizophrenia. Arch Gen Psychiat 1995 Dec 1;52(12):998-1007.

36. du Bois TM, Huang XF. Early brain development disruption from NMDA receptor hypofunction: relevance to schizophrenia. Brain Res Rev 2007 Feb 1;53(2):260-70.

37. Karoum F, Chrapusta SJ, Egan MF. 3-Methoxytyramine is the major metabolite of released dopamine in the rat frontal cortex: reassessment of the effects of antipsychotics on the dynamics of dopamine release and metabolism in the frontal cortex, nucleus accumbens, and striatum by a simple two pool model. J Neurochem 1994 Sep 1;63(3):972-9.

38. Gogos JA, Morgan M, Luine VV, Santha MM, Ogawa SS, Pfaff D, Karayiorgou M. Catechol-O-methyltransferase-deficient mice exhibit sexually dimorphic changes in catecholamine levels and behavior. Proc Natl Acad Sci USA 1998 Aug 17;95(17):9991-6.

39. Simpson EH, Morud J, Winiger V, Biezonski D, Zhu JP, Bach ME, Malleret G, Polan HJ, Ng-Evans S, Phillips PE, et al. Genetic variation in COMT activity impacts learning and dopamine release capacity in the striatum. Learn.Mem. 2014 Apr;21(4):205-14.

40. Yavich L, Forsberg MM, Karayiorgou M, Gogos JA, Mannisto PT. Site-specific role of catechol-O-methyltransferase in dopamine overflow within prefrontal cortex and dorsal striatum. J.Neurosci. 2007 Sep 19;27(38):10196-209.

41. Adams B, Moghaddam B. Corticolimbic dopamine neurotransmission is temporally dissociated from the

cognitive and locomotor effects of phencyclidine. J Neurosci 1998 Jul 15;18(14):5545-54.

42. Light GA, Swerdlow NR, Rissling AJ, Radant A, Sugar CA, Sprock J, Pela M, Geyer MA, Braff DL. Characterization of neurophysiologic and neurocognitive biomarkers for use in genomic and clinical outcome studies of schizophrenia. PLoS ONE 2012;7(7):e39434.

43. Gudlowski Y, Ozgurdal S, Witthaus H, Gallinat J, Hauser M, Winter C, Uhl I, Heinz A, Juckel G. Serotonergic dysfunction in the prodromal, first-episode and chronic course of schizophrenia as assessed by the loudness dependence of auditory evoked activity. Schizophr.Res. 2009 Apr;109(1-3):141-7.

44. Juckel G, Gudlowski Y, M++ller D, +ûzg++rdal S, Br++ne M, Gallinat J+, Frodl T, Witthaus H, Uhl I, Wutzler A, et al. Loudness dependence of the auditory evoked N1/P2 component as an indicator of serotonergic dysfunction in patients with schizophrenia GÇö A replication study. Psychiat Res 2008 Feb 1;158(1):79-82.

45. Wyss C, Hitz K, Hengartner MP, Theodoridou A, Obermann C, Uhl I, Roser P, Grunblatt E, Seifritz E, Juckel G, et al. The loudness dependence of auditory evoked potentials (LDAEP) as an indicator of serotonergic dysfunction in

patients with predominant schizophrenic negative symptoms. PLoS.One. 2013;8(7):e68650.

46. Schneider M, Van der Linden M, Glaser B, Rizzi E, Dahoun SP, Hinard C, Bartoloni L, Antonarakis SE, Debbane M, Eliez S. Preliminary structure and predictive value of attenuated negative symptoms in 22q11.2 deletion syndrome. Psychiatry Res. 2012 Apr 30;196(2-3):277-84.

47. Schneider M, Van der Linden M, Menghetti S, Debbane M, Eliez S. Negative and paranoid symptoms are associated with negative performance beliefs and social cognition in 22q11.2 deletion syndrome. Early Interv.Psychiatry 2015 Feb 26.

48. Stoddard J, Niendam T, Hendren R, Carter C, Simon TJ. Attenuated positive symptoms of psychosis in adolescents with chromosome 22q11.2 deletion syndrome. Schizophr.Res. 2010 May;118(1-3):118-21.

49. Rihs TA, Tomescu MI, Britz J, Rochas V, Custo A, Schneider M, Debbane M, Eliez S, Michel CM. Altered auditory processing in frontal and left temporal cortex in 22q11.2 deletion syndrome: a group at high genetic risk for schizophrenia. Psychiatry Res. 2013 May 30;212(2):141-9.

50. Van der Molen MJ, Van der Molen MW, Ridderinkhof KR, Hamel BC, Curfs LM, Ramakers GJ. Auditory change detection in fragile X syndrome males: a brain potential study. Clin Neurophysiol. 2012 Jul;123(7):1309-18.

51. Rotschafer S, Razak K. Altered auditory processing in a mouse model of fragile X syndrome. Brain Res 2013 Apr 19;1506:12-24.

52. Liao W, Gandal MJ, Ehrlichman RS, Siegel SJ, Carlson GC. MeCP2+/- mouse model of RTT reproduces auditory phenotypes associated with Rett syndrome and replicate select EEG endophenotypes of autism spectrum disorder. Neurobiol Dis 2012 Apr;46(1):88-92.

53. Graf R, Hanks A, Lotarski S, More LI, izzo SS, cott L, tolyar P, ughes ZA. Behavioral assessment of a mouse model of 22q11 deletion syndrome and its relevance to schizophrenia. Biol Psychiatry 2014;75(9):178S.

54. Wolf DH, Satterthwaite TD, Kantrowitz JJ, Katchmar N, Vandekar L, Elliott MA, Ruparel K. Amotivation in schizophrenia: integrated assessment with behavioral, clinical, and imaging measures. Schizophr.Bull. 2014 Nov;40(6):1328-37.

55. Stefansson H, Meyer-Lindenberg A, Steinberg S, Magnusdottir B, Morgen K, Arnarsdottir S, Bjornsdottir G,

Walters GB, Jonsdottir GA, Doyle OM, et al. CNVs conferring risk of autism or schizophrenia affect cognition in controls. Nature 2014 Jan 16;505(7483):361-6.

56. Giovanoli S, Engler H, Engler A, Richetto J, Voget M, Willi R, Winter C, Riva MA, Mortensen PB, Feldon J, et al. Stress in puberty unmasks latent neuropathological consequences of prenatal immune activation in mice. Science (New York N.Y.) 2013 Mar 1;339(6123):1095-9.

57. Sobin C, Kiley-Brabeck K, Monk SH, Khuri J, Karayiorgou M. Sex differences in the behavior of children with the 22q11 deletion syndrome. Psychiatry Res 2009 Mar 31;166(1):24-34.

Table 1

Model		Df(h22q11)/+	Df(16)A+/-	LgDel	Df1/+	
	Deletion	Dgcr2-Hira	Dgcr2-Hira	Dgcr2-Hira	Dgcr14-Ufd11	Znf74-Ctp
	Strain	C57/Bl6N	C57/Bl6J	C57/Bl6N	Mixed C57/Bl6C-/C-; 129S5/SvEvBrd	129SvEvTac or mixed 129SvEvTac
Phenotype	**Measure**					
PPI and startle	**Pre-pulse inhibition**					
	Pre-puberty	↓	-	-	-	-
	Post-puberty	↓	↓[16]	↓[14]	↓[15]	↑[24]
	Clozapine or haloperidol	X	-	-	-	-

	challenges					
	Acoustic startle					
	Pre-puberty	↑	–	–	–	–
	Post-puberty	↑	X[15]	↑[14]	↑[15]	X[24]
	Clozapine or haloperidol challenges	X	–	–	–	–
Stimulant	**PCP**					
LMA						
	Pre-puberty	X	–	–	–	–
	Post-puberty	↑	–	–	–	–
	Ketamine (post-puberty)	↑	–	–	–	–
Electrophysiology	**Prefrontal spike frequency**					
	Baseline	X	–	–	–	–
	Gabazine Challenge	X	–	–	–	–
	Cortical low frequency					

	oscillation					
	Baseline	X	–	–	–	–
	PCP challenge	X	–	–	–	–
	LDAEP	↑	–	–	–	–
	ABR	x	–	–	↓[17]	–
Biochemistry	**HPLC (PFC and DStr)**					
	DOPAC	↑	–	–	–	–
	DA, 5-HT, NA, 5-HIAA, HVA	x	–	–	–	–
	DStr microdialysis					
	Baseline DA, DOPAC, Glu, HVA	X	–	–	–	–
	Veratridine, nomifensine, PCP challenge	X	–	–	–	–
	Western analysis (PFC, DStr, Hipp)					
	Synaptic (PSD-95, SYP,	X	–	–	–	–

Syn1, Drebrin, geophysin)					
Cell type (NeuN, GFAP)	X	-	-	-	-
GABA (GABAAα1, KCC2, VGAT, GAD65/67)	X	-	-	-	-
Glutamate (GluR2, NR2A, NR2B, VGluT1)	X	-	-	-	-
DStr GluR1	↑	-	-	-	-

Table 1. Summary of results for Df(h22q11)/+ and other 22q11.2DS mouse models. ↓ decreased, ↑ increased, x no effect, - no data. LMA = Locomotor activity; PFC = prefrontal cortex; DStr = dorsal striatum; Hipp = hippocampus; LDAEP = loudness dependence auditory evoked potentials; ABR = auditory induced brainstem response.

Table 2

Type	**Marker**	**Function**	**PFC**	**DStr**	**Hipp**
Synaptic	PSD-95	Scaffolding protein at excitatory post synaptic densities	x	x	x
	Synaptophysin	Synaptic vesicle protein	x	x	x
	Synapsin 1	Phosphoprotein associated with surface of synaptic vesicles	x	x	x
	Drebrin	Actin-binding protein involved in neuronal /spine growth	x	x	x
	Gephyrin	Scaffolding protein in inhibitory synaptic densities	x	x	x
Cell type	NeuN	Nuclear antigen. Biomarker of neurons	(↓)	x	x
	GFAP	Intermediate filament in astrocytes	x	x	x
Glutamate	GluR1	AMPA receptor	x	↑	x

		subunit			
	GluR2	AMPA receptor subunit	x	x	x
	NR2A	NMDA receptor subunit	x	x	x
	NR2B	NMDA receptor subunit	x	x	x
	VGluT1	Vesicular glutamate transporter at vesicle membrane	x	x	x
GABA	GABAA α1	$GABA_A$ receptor subunit	x	x	x
	KCC2	Neuron specific potassium-chloride transporter	x	x	x
	VGAT	Vesicular GABA transporter found on synaptic vesicle membrane	x	x	x
	GAD 65/6	Enzymes catalysing decarboxylation of glutamate to GABA	x	x	x

Table 2. Protein level in Df(h22q11)/+ and WT littermates ↓ decreased, ↑ increased, x no effect. () did not replicate. PFC = prefrontal cortex, DStr = dorsal striatum, Hipp =

hippocampus.

Figure 1

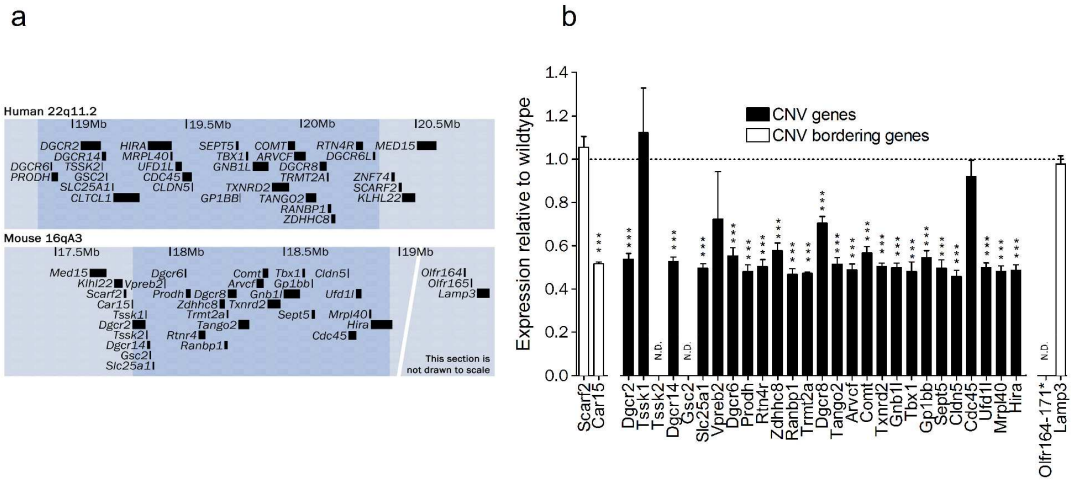

Figure 1. Construct similarities in Df(h22q11)/+ and human deletion carriers. **(a)** Overview of the deleted region (shaded) in human (22q11.2) and the corresponding orthologous region in mouse (16qA3). The maps are based on human library GRCh38/hg38 and mouse library GRCm38/mm10 from the UCSC database. Only annotated RefSeq sequences are shown for clarity. **(b)** Median normalized microarray analysis of relative cortical expression of gene products from deleted segment in Df(h22q11)/+ compared with WT littermates. Asterisk denote significant difference between WT and Df(h22q11)/+ (***p< 0.001). N.D.: not detected.

Figure 2

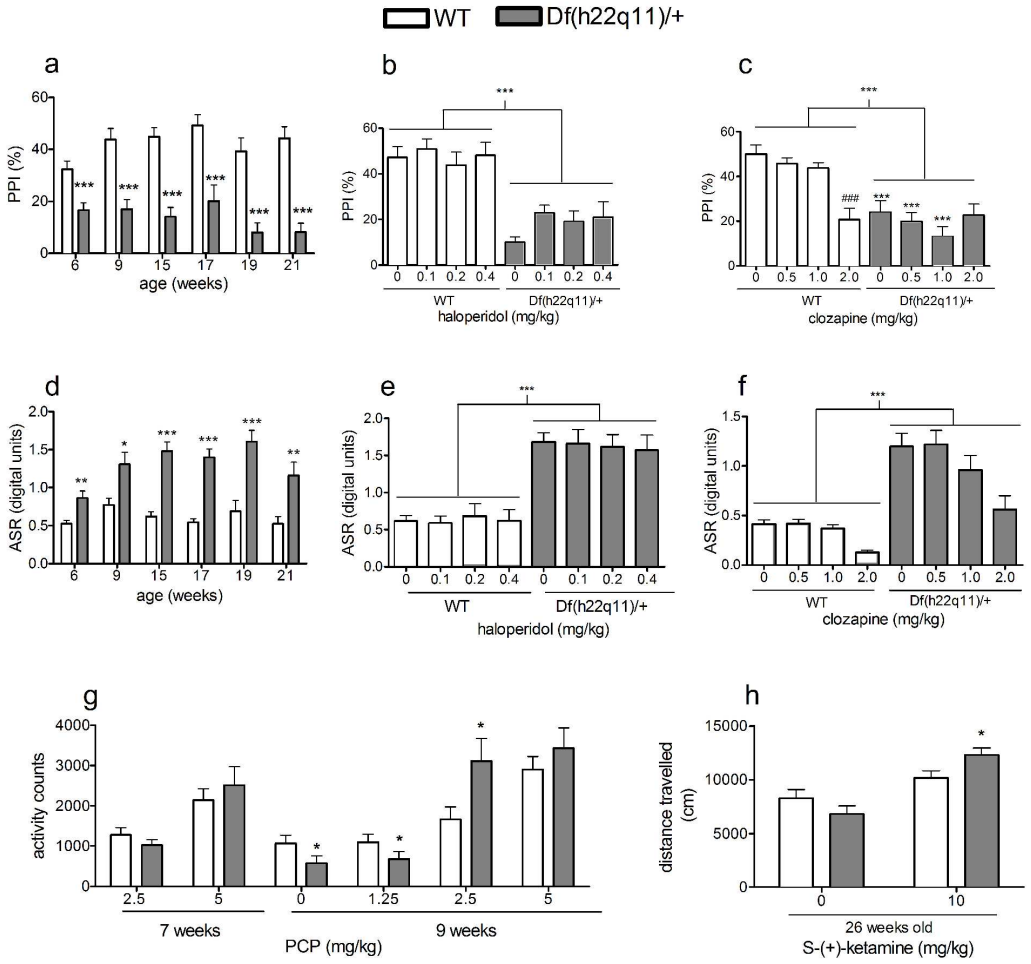

Figure 2. Behavioural characterisation of Df(h22q11)/+ and WT littermates. (**a) Pre-pulse inhibition (PPI).** Df(h22q11)/+ mice showed decreased PPI. The PPI deficit was reproduced in 6 independent cohorts 6-21 weeks of age (n = 12-24/group) (t-test was conducted for each week; W6: t_{45} = 3.6, p<0.001; W9: t_{30} = 4.8, p<0.001; W15: t_{29} = 6.3, p<0.001; W17: t_{22} = 3.9, p<0.001; W19: t_{22} = 4.9, p<0.001; W21: t_{22} = 6.4, p<0.001). **(b) PPI – effect of haloperidol.** Haloperidol did not rescue the PPI deficit (n = 12/group) (2-way ANOVA; genotype: $F_{1,94}$ = 69.1, p <

0.001; dose: $F_{3,94}$ = 1.02, p = 0.38; genotype×dose: $F_{3,94}$ = 0.59, p = 0.63). **(c) PPI – effect of clozapine.** Clozapine did not rescue the PPI deficit (n=13/group) (2-way ANOVA; genotype: $F_{1,87}$ = 46.3, p < 0.001; dose: $F_{3,87}$ = 4.87, p = 0.004; genotype×dose: $F_{3,87}$ = 6.14, p < 0.001). **(d) Acoustic startle response (ASR).** Df(h22q11)/+ mice had increased ASR. The increased ASR was found in 6 independent cohorts 6-21 weeks of age (n = 12-24/group) (t-test was conducted for each week; W6: T = 418, p = 0.004; W9: T = 204, p = 0.025; W15: T = 340, p<0.001; W17: T = 79, p<0.001; W19: t_{22} = -4.51, p<0.001; W21: T = 101, p = 0.005). **(e) ASR – effect of haloperidol.** Haloperidol did not attenuate the increased ASR (n = 12/group) (2-way ANOVA; genotype: $F_{1,94}$ = 88.5, p < 0.001; dose: $F_{3,94}$ = 0.060, p = 0.98; genotype×dose: $F_{3,94}$ = 0.13, p = 0.95). **(f) ASR – effect of clozapine.** Clozapine did not attenuate the increased ASR (n = 13/group) (2-way ANOVA; genotype: $F_{1,87}$ = 83.1, p < 0.001; dose: $F_{3,87}$ = 9.35, p < 0.001; genotype×dose: $F_{3,87}$ = 1.49, p = 0.22). **(g) PCP-induced locomotor activity.** Age-dependent hypersensitivity to PCP-induced locomotion in Df(h22q11)/+ mice (n = 12/group) (t-test was conducted for each week; W7: t_{22} = 1.10, p = 0.28 at 2.5 mg/kg; t_{22} = -0.68, p = 0.50 at 5.0 mg/kg; W9: T = 90, p = 0.011 for vehicle; T = 187, p = 0.035 at 1.25 mg/kg; t_{22} = -2.33, p = 0.029 at 2.5 mg/kg; t_{22} = -0.91, p = 0.37 at 5.0 mg/kg). **(h) Ketamine-induced locomotion.** Hypersensitivity to ketamine induced locomotion in Df(h22q11)/+ mice (n = 13-16/group) (2-way ANOVA; genotype: $F_{1,54}$ = 0.23.1, p

= 0.64; dose: $F1_{1,54}$ = 25.6, p < 0.001; genotype×dose: $F_{1,54}$ = 5.95, p = 0.018; post hoc within ketamine 10 mg/kg t = 2.05, p = 0.044). Data are presented as mean + SEM. Asterisk denote significant differences between WT and Df(h22q11)/+ (*p < 0.05, **p< 0.01, ***p< 0.001). # denote significant difference within genotype relative to vehicle ($^{\#}$p < 0.05, $^{\#\#\#}$p< 0.001).

Figure 3

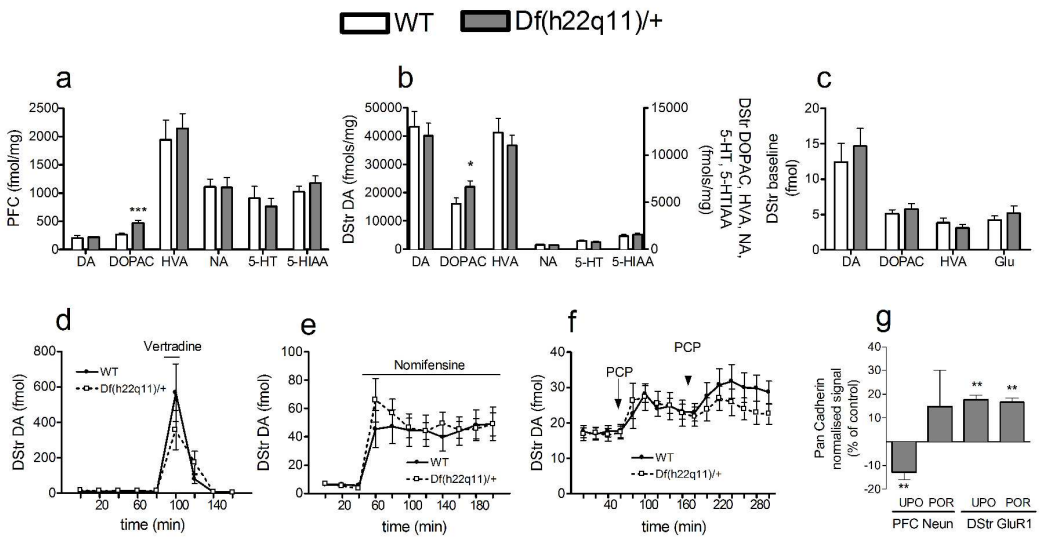

Figure 3. Biochemical measures in Df(h22q11)/+ and WT littermates. **(a) PFC whole tissue content.** The level of DOPAC was increased in Df(h22q11)/+ mice (n = 8-10/group) (t-test was conducted for each analyte; DA: t_{16} = -0.22, p = 0.83; DOPAC: t_{16} = -3.85, p = 0.001; HVA: t_{16} = -0.48, p = 0.64; NA: T = 81, p = 0.69; 5-HT: T = 83, p = 0.56; 5-HIAA: t_{16} = -0.93, p = 0.38 **(b) DStr whole tissue content.** The level of DOPAC was increased in Df(h22q11)/+ mice (n = 9-15/group) (t-test was conducted for each analyte; DA: t_{27} = 0.45, p = 0.66; DOPAC: T = 156, p = 0.020; HVA: T = 215, p = 0.84; NA:T = 238, p = 0.85; 5-HT: t_{28} = 0.91, p = 0.37; 5-HIAA: T = 198, p = 0.16. **(c) Microdialysis - DStr baseline.** No genotype effect (n = 14-15/group) (t-test was conducted for each analyte; DA: T = 203, p = 0.52; DOPAC: t_{27} = -0.69, p = 0.50; HVA: t_{19} = 0.98, p =

0.34; Glu:T = 191, p = 0.58). **(d) Effect of local veratridine application on DStr DA release.** Veratridine increased DStr DA similarly in WT and Df(h22q11)/+ mice (n = 14/group) (2-way RM ANOVA; genotype: $F_{1,26}$ = 0.24, p = 0.63; time: $F_{8,208}$ = 18.8, p < 0.001; genotype×time: $F_{8,208}$ = 1.35, p = 0.22). **(e) Effect of local nomifensine application on DStr DA release.** Nomifensine increased DStr DA similarly in WT and Df(h22q11)/+ mice (n = 14/group) (2-way RM ANOVA; genotype: $F_{1,26}$ = 0.12, p = 0.74; time: $F_{10,260}$ = 25.5, p < 0.001; genotype×time: $F_{10,260}$ = 0.79, p = 0.64). **(f) Effect of PCP on DStr DA release.** PCP increased DStr DA similarly in WT and Df(h22q11)/+ mice (n = 14/group) following both the first (genotype: F1,28 = 0.003, p = 0.958; genotype×time: $F_{4,112}$ = 0.742, p = 0.565) and second PCP challenge (genotype: $F_{1,28}$ = 1.632, p = 0.212; genotype×time: $F_{5,140}$ = 0.432, p = 0.826).**(g) Western analyses.** The initial analysis show decreased PFC NeuN (t_{20} = 2.92, p = 0.009) and increased DStr GluR1 expression (t_{20} = 2.99, p = 0.007) in Df(h22q11)/+ mice (n = 11/group). However, the NeuN decrease failed to replicate when samples were pooled. Data are presented as mean + SEM or mean ± SEM. Asterisk denote significant differences between WT and Df(h22q11)/+ (*p < 0.05, **p< 0.01). DA (dopamine); DOPAC (3,4-Dihydroxyphenylacetic acid); HVA (homovanillic acid); NA (norepinephrine); 5-HT (5-hydroxytryptamine); 5-HIAA (5-Hydroxyindoleacetic acid). VTD (veratridine); UPO (unpooled); POR (pooled replication); DStr (dorsal striatum).

Figure 4

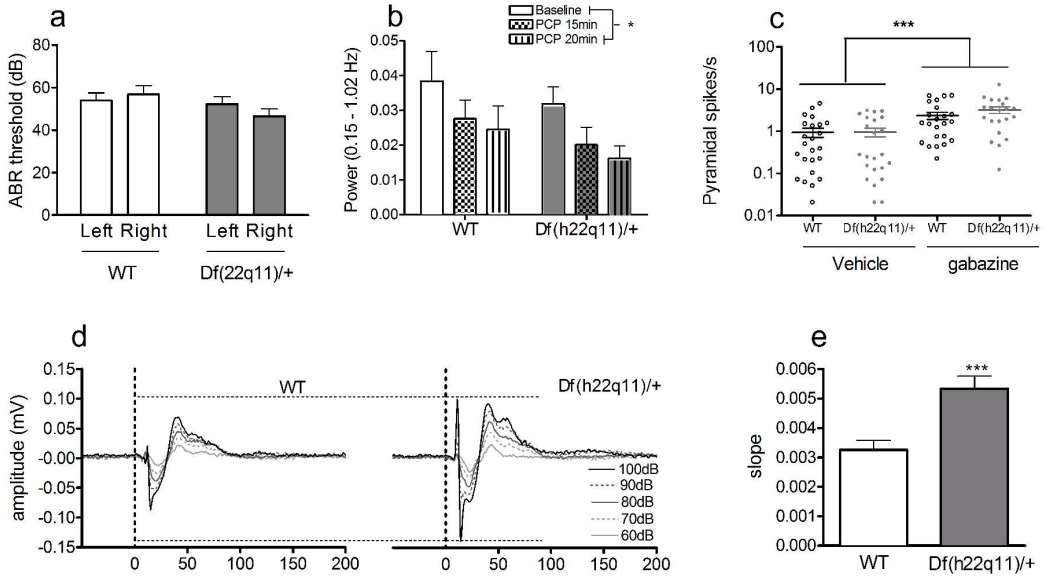

Figure 4. Electrophysiological measures in Df(h22q11)/+ and WT littermates. **(a) Auditory brain stem response (ABR).** The hearing in the Df(h22q11)/+ mice was not different from WT (n = 13/group) (2-way RM ANOVA; genotype: $F_{1,24}$ = 1.649, p = 0.211; ear: $F_{1,24}$ = 0.331, p = 0.571; ear×genotype: $F_{1,24}$ = 3.570, p = 0.071). **(b) PCP induced attenuation of cortical low frequency oscillations (LFO).** PCP caused similar decrease of cortical LFOs in WT and Df(h22q11)/+ mice (n = 9/group) (2-way ANOVA; genotype: $F_{1,48}$ = 2.40, p = 0.13; condition: $F_{2,48}$ = 3.44, p = 0.040; genotype×condition: $F_{2,24}$ = 0.013, p = 0.99). **(c) Gabazine-induced elevation of mPFC pyramidal spike frequency.** Gabazine caused similar increase in pyramidal spike frequencie in WT and Df(h22q11)/+ mice (n = 14/group) (2-way ANOVA; genotype: $F_{1,87}$ = 1.21, p = 0.28; treatment: $F_{1,87}$ = 20.9, p <

0.001; genotype×treatment: $F_{1,87}$ = 1.12, p = 0.29). **(d) LDAEP waveforms.** Grand average LDAEP waveforms from AuC in WT and Df(h22q11)/+ mice (n = 22-23/group) (2-way RM ANOVA; P1/N1:genotype: $F_{1,43}$ = 22.6, p < 0.001; intensity: $F_{4,43}$ = 75.5, p < 0.001; genotype×intensity: $F_{4,43}$ = 13.7, p < 0.001; N1/P2: genotype: $F_{1,43}$ = 9.89, p = 0.003; intensity: $F_{4,43}$ = 156.4, p < 0.001; genotype×intensity: $F_{4,43}$ = 9.76, p < 0.001). **(e) LDAEP slope.** Collapsed LDAEP slopes for Df(h22q11)/+ and WT mice (n=22-23/group) (t-test; t_{43} = -3.896, p < 0.001). Data are presented as mean + SEM or mean ± SEM. Asterisks denote significant differences (*p < 0.05, ***p< 0.001).

Supplementary material for

Persistent gating deficit and increased sensitivity to NMDA receptor antagonism after puberty in a new mouse model of the human 22q11.2 micro-deletion syndrome

M Didriksen[1], K Fejgin[1], SRO Nilsson[2,3], MR Birknow[1], HM Grayton[4], PH Larsen[1], JB Lauridsen[1], V Nielsen[1], P Celada[5], N Santana[6], P Kallunki[1], KV Christensen[1], TM Werge[7], TB Stensbøl[1], J. Egebjerg[1], F Gastambide[4], F Artigas[5,6], JF Bastlund[1], J Nielsen[1]

[1]H. Lundbeck A/S, Neuroscience Research DK, Ottiliavej 9, Valby 2500, Denmark.[2]Department of Psychology, University of Cambridge, Cambridge, CB2 3EB, UK. [3]Behavioural and Clinical Neuroscience Institute, University of Cambridge, Cambridge, CB2 3EB, UK. [4]Lilly Centre for Cognitive Neuroscience, Lilly Research Laboratories, Eli Lilly & Co. Ltd, Erl Wood Manor, Sunninghill Road, Windlesham, GU20 6PH, UK. [5]Institut d'Investigacions Biomèdiques de Barcelona, CSIC-IDIBAPS, Barcelona, Spain. [6]Centro de Investigación Biomédica en Red de Salud Mental (CIBERSAM), Spain. [7]Institute of Biological Psychiatry, MHC Sct. Hans, Copenhagen Mental Health Services; Institute of Clinical Sciences, Faculty of Medicine and Health Sciences, University of Copenhagen;

iPSYCH - The Lundbeck Foundation's Initiative for Integrative Psychiatric Research, Boserupvej, DK-4000 Roskilde, Denmark

Supplementary methods

Animals

Generation of the Df(h22q11)/+ mouse (Figure A1)

The mouse construct was generated using two targeting vectors. The first vector introduced a loxP site with an FRT-flanked Neomycin resistance cassette upstream of exon 9 in the Dgcr2 gene. The second vector introduced a loxP site with an F3-flanked Puromycin resistance cassette downstream of exon 24 in the Hira gene. Both constructs also contained a thymidine kinase gene for negative selection. Targeted sequences were generated using BAC clones from the C57BL/6J RPCI-23 BAC library. First, linearized Dgcr2-targeting vectors were electroporated into the TaconicArtemis C57BL/6N Tac embryonic stem cell (ESC) line. Homologous recombinant clones were isolated by positive (G418 resistance) and negative (Gancyclovir resistance) selection. The genetic construct was validated by southern blotting to confirm a single integration on only one chromosome. Secondly, selected ESC lines were electroporated with linearized Hira-targeting vector. Homologous recombinant clones were isolated using positive (puromycin resistance) and negative (Gancyclovir resistance) selection. Again, the genetic construct was validated by southern blotting to confirm a single integration on only one chromosome. Thirdly, double targeted ESC lines were electroporated with a cre-recombinase expressing construct to facilitate in vitro Cre-

mediated recombination in ESC clones with the two loxP sites inserted on the same chromosome. The ESCs hemizygotic for the 1.13Mb deletion were identified by southern blotting and polymerase chain reaction (PCR) analysis. The final construct had section 17,840,564 – 18,970,580 (a 1,129,815 basepair deletion) exchanged with a 101 basepair sequence containing a loxP site on chromosome 16 as mapped to reference sequence NC_000082.6 from the GRCm38/mm10 library. Finally, selected ESCs were microinjected into blastocysts isolated from impregnated BALB/c females and transferred to pseudopregnant NMRI females. Chimeric male pups were selected by coat colour and mated with WT C57BL/6N females and a chimera with germline transmission was selected for expansion breeding. Genotypes were controlled during breeding by PCR on tail biopsies.

Confirmation of the transcriptional levels (Figure 1b)

To confirm the transcriptional changes of the genetic construct, tissue was isolated from the frontal part of the cortex by hand dissection and shipped for RNA extraction and microarray analysis at Miltenyi Biotec, Germany. In brief, RNA was isolated using standard RNA extraction protocols (Trizol) and quality-checked via the Agilent 2100 Bioanalyzer platform (Agilent Technologies, RNA integrity values were between 7.2 and 9.1). 100ng of each sample was used for a linear T7-based amplification step to produce Cy3-labeled cRNA using the Agilent Low Input Quick Amp Labeling Kit (Agilent Technologies) according

to manufacturer. 600ng of Cy3-labeled fragmented cRNA was then hybridized to Agilent 8x60K Whole Mouse Genome Oligo Microarrays overnight (17 hours, 65°C) according to the Agilent 60-mer oligo microarray processing protocol using the Agilent Gene Expression Hybridization Kit (Agilent Technologies). Finally, the microarrays were washed and read using Agilent's Microarray Scanner System. Scanned images were processed using the Agilent Feature Extraction Software (FES) which determines feature intensities (including background subtraction), rejects outliers and calculates statistical confidences. Normalized signal intensities were obtained by dividing each value by the median value of each array. Genes close to the deleted region were included for detection of possible effects on bordering genes. The number of genes upstream and downstream of the deleted region was increased until transcripts could be detected in WT cortex above background levels (based on FES). Significance levels are based on two-tailed t-test with Welsh correction. Data presented as expression in the Df(h22q11)/+ relative to WT.

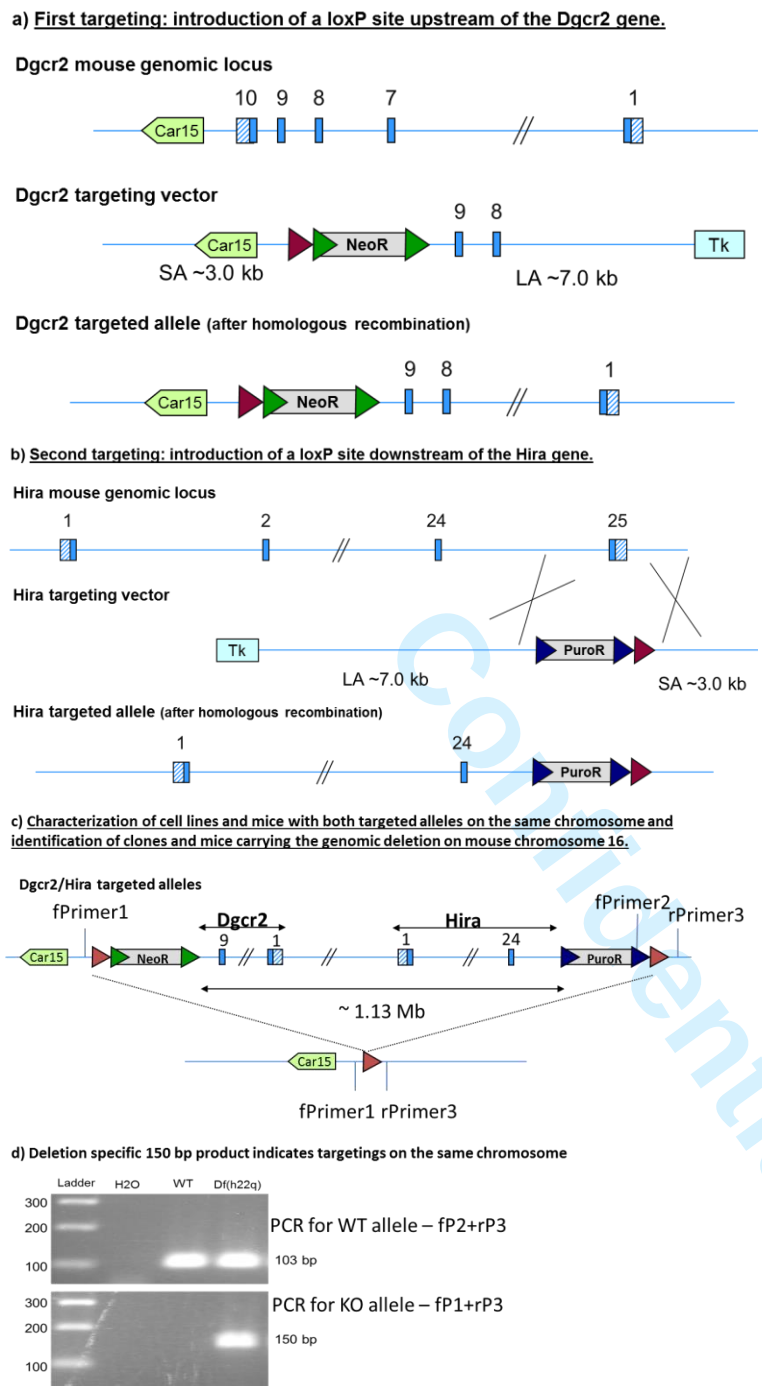

Supplementary Figure A1. Generation of Df(h22q11) mice. A) WT Dgcr2 loci and the corresponding targeted loci following introduction of a lox P site and Neomycin resistance gene. B). WT Hira loci and the corresponding targeted loci following introduction of a lox P site and Puromycin resistance gene. C)

Cre-induced recombination between loxP sites in cis leads to around 1.13-Mb deficiency, leaving only a single Lox P site. Deletion specific oligonucleotides used for PCR analysis are indicated around the Lox P sites D) Due to the recombination of the loxP sites, a diagnostic 150-bp PCR product can be detected in Df(h22q11) mice. The 103 bp PCR product is internal control to show that DNA is present in all samples. Diagrams are not drawn to scale.

Behaviour

For the age at the start of each experiment and the distribution of the 27 cohorts of Df(h22q11)/+ and WT littermates used for the studies please refer to Figure A2 below.

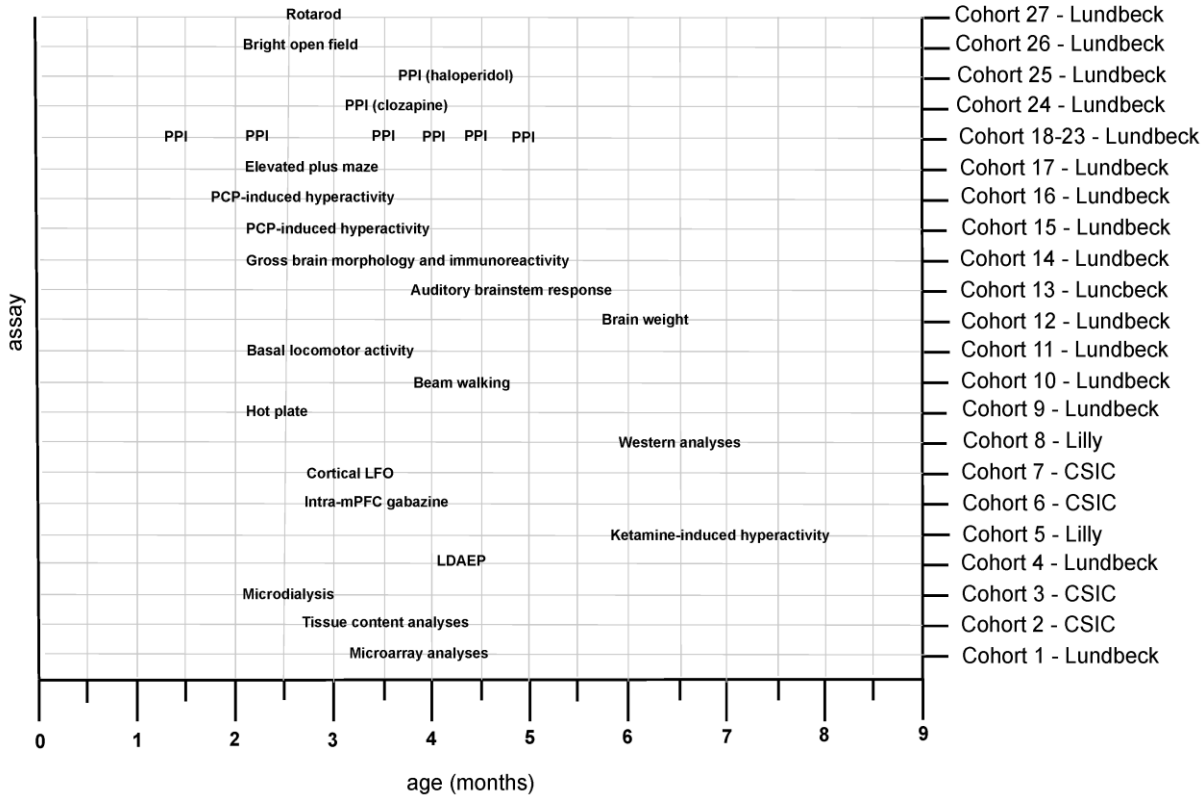

Supplementary Figure A2. Cohort 1 was used for PFC microarray analyses (WT N = 12, TG N = 5). Cohort 2 was used for whole tissue content analyses (PFC: WT N = 8, TG N = 10; DStr: WT N = 14/15, TG N = 15). Cohort 3 was used for microdialysis experiments (WT N = 14, TG N = 14). Cohort 4 was used for LDAEP analyses (WT N = 22; TG N = 23). Cohort 5 was used for ketamine-induced hyperactivity (WT N = 13, TG N = 16). Cohort 6 (WT N = 14, TG N = 14) was used for the intra-mPFC gabazine experiment. Cohort 7 (WT N = 9; TG N = 9) was used for the cortical LFO experiment. Cohort 8 was used for western analyses (WT N = 11; TG N = 11). Cohort 9 was used for hot plate (WT N = 12, TG N = 12). Cohort 10 was used for beam walking (WT N = 16; TG N = 16). Cohort 11 was used for basal LMA (WT N = 48; TG N = 47). Cohort 12 was used for brain weight (WT N = 9; TG N = 9). Cohort 13 was used for auditory brainstem response analyses (ABR; WT N = 13; TG N = 13). Cohort 14 was used for gross histological and immunoreactivity studies (WT N = 6; TG N = 6). Cohort 15 and

Cohort 16 (WT Ns = 12; TG Ns = 12) was used for PCP-induced hyperactivity. Cohort 17 was used for elevated plus maze (WT N = 12; TG N = 12). Cohort 18 (WT N = 23; TG N = 24), Cohort 19 (WT N = 16; TG N = 16), Cohort 20 (WT N = 16; TG N = 15), Cohort 21, Cohort 22, and Cohort 23 (WT Ns = 12; TG Ns = 12) were used for PPI. Cohort 24 (WT N = 13; TG N = 13) and Cohort 25 (WT N = 12; TG N = 12) were used for haloperidol- and clozapine-challenged PPI experiments. Cohort 26 (WT N = 16; TG N = 16) was used for the bright open field. Cohort 27 (WT N = 10; TG N = 10) was used for the rotarod experiment. CSIC = Consejo Superior de Investigaciones Científicas, Barcelona.

Beam-walking (Figure A3i)

The day before testing, all mice were individually trained to traverse a narrow beam (16 mm wide 75 cm long) at a height of 30 cm to reach a dark enclosure. The beam walking test was performed in daylight the following day, using a thinner test beam (8 mm wide). Each animal was observed for foot slips, falls and time to cross the beam.

Rotarod (Figure A3e)

The rotarod test was performed using a Rotamex 4/8 (Columbus Instruments, 950N. Hague Avenue, Columbus, Ohio 43204 USA), equipped with 2x4 lanes and 75 mm rods. A paradigm accelerating from 4 - 40 rpm within 5 min, and a detection delay set to 0 seconds, was used. Each mouse was tested in the paradigm 3 times / day with a 20 min break between each trial for 4 consecutive days. The Columbus instruments special designed software automatically calculated the accumulated time-on-the-rod. Both maximum latency (best performance of the day) and average latency each day to fall off the rotating rod was scored for each session.

Locomotor activity (Figure A3d)

Mice were placed individually in macrolon locomotor activity cages (20 cm × 35 cm × 18 cm) to habituate for 60 min and basal locomotor activity was measured. The locomotor activity cages were equipped with 5 × 8 infrared light sources and photocells. The light beams crossed the cage 1.8 cm above the bottom of the cage. To avoid stationary movement artefacts, two consecutive crossings of adjacent infrared light beams were recorded as a motility count. Registration and timing of locomotor activity was fully automated (custom-designed hardware and software by Ellegaard Systems A/S, Faaborg, Denmark).

NMDAr antagonist induced activity (Figure 3g-h)

PCP study. Mice were placed individually in macrolon locomotor activity cages (20 cm × 35 cm × 18 cm) to habituate for 60 min. After the habituation period, vehicle or PCP (1.25, 2.5 or 5.0 mg/kg, s.c., 10 ml/kg) was administered and locomotor activity was recorded for an additional 60 min. The locomotor activity cages were equipped with 5 × 8 infrared light sources and photocells. The light beams crossed the cage 1.8 cm above the bottom of the cage. To avoid stationary movement artefacts, two consecutive crossings of adjacent infrared light beams were recorded as a motility count. Registration and timing of locomotor activity was fully automated (custom-designed hardware and software by Ellegaard Systems A/S, Faaborg, Denmark).

Ketamine study. The study was conducted in complete dark test rooms, using clear Perspex boxes (40×40×30 cm) which were placed on infrared fields (100×100 cm), four boxes per field. Locomotor activity was monitored using overhead infrared cameras (Sanyo VCV-3412P, TrackSys Ltd, UK), that fed into a PC running the image analysis application Ethovision v2.2 (Noldus, NL). Mice were assigned to treatment groups/sequence using a pseudorandomised block method where treatments were balanced across the time of day, the test room and the week of testing. On

each test day, mice were placed individually into the test boxes to habituate for 60 min. After the habituation period, vehicle or S-(+)-ketamine (10 mg/kg, s.c., 10 ml/kg) was administered and locomotor activity was recorded for an additional 60 min.

Hotplate (Figure A3f)

The test was performed using Ugo Basile 7280 Hotplate system, (Ugo Basile, Biological Research Apparatus, 21025 Comerio VA Italy). Mice were individually placed in a glass cylinder on the heating plate with a fixed temperature. Latency time to lifting one limb or jumping was measured. Each mouse was tested 3 times at increasing temperature levels 50, 53 and 56 °C with 30 min break between each test. Average latency time was calculated for each temperature level.

Bright open field (Figure A3h)

Individual mice were placed in a bright illuminated (120 lux) circular open field (74 cm diameter). Activity was measured for one hour by a camera installed above the arena. Movement and position was automatically video tracked and quantified into 3 predefined zones; Center (25 cm diameter), middle (12.5 cm band) and outer (12.5 cm band) using the Ethovision 7.0 software (Noldus Information Technologies, Wageningen, the Netherlands).

Elevated plus maze (Figure A3g)

The elevated plus maze setup, consisted of a grey plus-shaped maze with 2 open arms and 2 arms with side walls, also referred to as closed arms (arm dimension 17x8 cm). The maze was elevated 40cm above the floor, with an infrared camera installed above. The test was performed in darkness (2-5 lux).
Mice were individually placed in the centre of the maze and allowed to explore for 5 min. Movement and position was automatically video tracked and quantified into time spent on open vs. closed arms and number of entries into zones (defined by

head and forelimbs entered into the zone), using the Ethovision 7.0 software (Noldus Information Technologies, Wageningen, the Netherlands).

Prepulse inhibition (PPI) (Figure 2a-f)

PPI testing was performed using the SM100 Startle Monitor System (Kinder Scientific, USA), consisting of 8 sound-attenuated startle chambers and StartleMonitor software (Kinder Scientific, USA). Animals were placed in an adjustable Plexiglas holder, providing limited movement but not restraint, positioned directly above a sensing platform registering the animals startle response. Each test session consisted of a 5 min acclimatization period with only background white noise (62 dB), followed by a brief habituation setting where 32 regularly occurring startle pulses of 105 dB (intertrial interval (ITI): 10 s) were presented to the animals to maximize habituation prior to the PPI part of the session. Animals were then subjected to 5 types of trials presented 12 times each in a balanced manner: pulse alone, prepulse + pulse (5, 10 or 15 dB above background), or highest prepulse intensity (77 dB) alone. ITI varied between 9 and 21 s (average ITI 15 s) and inter-stimulus interval (ISI) was set to 100 ms with a prepulse length of 20 ms. Each PPI session ended with 8 startle pulses of 105 dB to estimate habituation across PPI trials. The full PPI test lasted about 28 min. PPI was calculated as % PPI for each prepulse intensity as: 100 – ((prepulse + pulse/pulse alone) × 100), i.e. a lower percentage score indicates a decrease in PPI. Startle magnitude was calculated as an average of pulse alone trials.

Electrophysiology

Loudness dependence auditory evoked potentials (Figure 4)

Surgical procedures. Epidural screw electrodes (Plastic One, Virginia) were placed according to coordinates from Franklin and

Paxinos(1) at the following positions relative to bregma in the auditory cortex (AP: -2.92 mm, ML: -4.25 mm), frontal cortex (AP: +2.8, ML: -0.5 mm), parietal cortex corresponding to the vertex (AP: -2.0, ML: -2.0 mm), reference (AP: -6.0, ML: +2.0 mm) and ground (AP: -2.0, ML: +2.5 mm). A teflon-coated stainless steel depth electrode (0.125 mm, Plastic One, Virginia) was placed in the hippocampus (CA1) at (AP: -3.16, ML: -3.2, DV: -1.4 mm to dura). The location of the hippocampal depth electrode was verified by histological inspection. Electrodes were connected to a 6-channel pedestal (Plastic One, Virginia), which was fixated to the skull with dental cement (GC Fuji PLUS Capsule, GC Corporation, Japan). Post-surgery, mice were housed individually and allowed minimum of two weeks recovery including five days of handling and one day of habituation to the test environment without (1 h) and with auditory stimulation (2h). In the post-surgical period, the circadian rhythm of the mice was reversed (12 hours of light starting at 6 pm) to allow electrophysiological experiment to be performed during the dark phase (active phase). On test days, mice were habituated to the test environment for 2 h prior to auditory testing.

Electroencephalography (EEG) recordings. EEG was recorded in WT and Df(h22q11)/+ mice during the dark phase by connecting a custom made 6-channel cable attached to a 10-channel commutator (Dragonfly, USA) allowing the mice to move freely. EEG data was digitalised and collected at a sampling rate of 1000Hz (Power1401, Cambridge Electronic Design, Cambridge, UK) and amplified with gain x1000 and band-pass filtered using hardware filter at 1.0-300 Hz with an additional notch filter to remove 50 Hz noise (BrownLee, model 440, USA). Auditory stimuli generation and data analyses were done using the Spike 2 software package (v. 7.07; Cambridge Electronic Design, Cambridge, UK). Auditory stimulus was presented via two speakers in the side of the housing cages in custom made sounds attenuated faraday steel boxes. The sounds intensity was controlled by a custom made sound

attenuator (Ellegaard Systems, Denmark) and an amplifier (Tony Lee DJ201, JCLEON International Electronic, China).

Auditory brainstem response (Figure 4)

ABR measures evoked by click-stimuli from left and right ears were recorded in a sound-attenuating faraday cage. Mice were anaesthetised with ketamine/xylazine (0.1 ml/10 g of 10 mg ketamine/10 g and 0.1 mg xylazine/10 g; 10 ml/kg, i.p.) and placed in a stereotaxic frame with hollow ear bars guiding sound waves to the external auditory meatus. A heating pad maintained body temperature was during recordings. Subdermal needle electrodes (HUSH™ Shielded Electrode Cable, 3x0.7 mm female, 2 m; Dantec Disposable Scalp Needle Electrodes, 10 x 0.30 mm (30G); Natus Medical Incorporated, USA) were inserted under the skin with the active electrode at the vertex, the reference electrode at the ear being tested, and the ground electrode near the opposite ear. Biological signals were amplified (x1000), filtered (bandpass hardware filter: 1.0-8000 Hz; notch filter to remove 50 Hz noise) (BrownLee, model 440, USA) and digitalised at a sampling rate of 100.000 Hz (Power 1401, Cambridge Electronic Design, Cambridge, UK). Acoustic stimuli were generated by Spike 2 software (v. 7.07; Cambridge Electronic Design, Cambridge, UK), amplified (Argon Audio headphone amplifier, model HA1, Denmark) and presented through insert-earphones connected to hollow ear bars guiding the sound waves directly to the external auditory meatus. All tones were calibrated with a Bruel & Kjaer microphone (Sound level meter Type 2236; Microphone Type 4188) prior to ABR testing.

Gabazine and local field potentials (Figure 4)

Surgical procedures. Mice were anesthetized with chloral hydrate (400 mg/kg i.p, followed by a maintenance dose of ≈ 1 mg/kg/min i.p. using a perfusion pump). Body temperature was maintained at 37˚C using a heating pad. Single unit recordings

were carried out with glass micropipettes pulled from 2 mm capillary glass (World Precision Instruments, Sarasota, FL) on a Narishige (Tokyo, Japan) PE-2 pipette puller. Electrode descents were carried out in the mPFC at coordinates AP: + 2.1, L: -0.2-0.4, DV: -1-2.5 mm. Stereotaxic coordinates were taken from bregma and duramater according to the mouse brain atlas (1). The signal was amplified (x10) with a Neurodata IR283 (Cygnus Technology Inc., Delaware Water Gap, PA), postamplified (x100) and filtered (band pass filter 30 Hz-10 kHz for spikes and 0.1-100 Hz for local field potential) with a Cibertec amplifier/filter (Madrid, Spain) and computed using a DAT 1401plus interface system Spike2 software (Cambridge Electronic Design, Cambridge, UK). At the end of experiments, mice were sacrificed by decapitation, the brains rapidly removed and prefrontal cortex (PFC) and caudate putamen (CP) dissected out on an ice-cold plate. Tissue samples were frozen at -20°C until analysed.

Gabazine experiment. Spontaneous discharge rate of putative pyramidal neurons was analysed in control conditions and during local blockade of $GABA_A$-Rs with the selective antagonist gabazine (SR95531, Sigma-Aldrich, St Louis, MO). Electrodes were filled with saline 2 M (impedances: 6-12 MΩ) or gabazine (20 mM) dissolved in 0.2 M NaCl. Gabazine was preferred to the classical $GABA_A$ antagonist bicuculline due to the non-selective action of the latter agent (2). Electrode tips were broken to a final resistance of 9-15 MΩ (electrode tip: 5-7µm diameter). Gabazine leaked from the recording electrode by passive diffusion to reach the recorded neuron, as shown previously for bicuculline (3;4). The onset of drug effects was very rapid, usually >10 s. Once a putative pyramidal neuron was encountered, a ≤ 5 min recording was made to obtain a reliable measure of spontaneous discharge rate after which the electrode was descended again.

Local field potential recordings. Local field potential (LFP) recordings were performed in basal conditions and following

acute PCP treatment (10 mg/kg s.c., Sigma-Aldrich, Madrid, Spain). Off-line analysis was performed using the Spike 2 software (Cambridge Electronic Design, Cambridge, UK). Power spectra were constructed by using Fast Fourier Transformation (FFT) of 1 min signal intervals (band-pass filter of 0.1-100 Hz) corresponding to baseline and PCP. Power resolution was 0.15 Hz. Results are presented as AUCs.

Anatomy and biochemistry

Gross anatomical and histological analyses (Figure A4)

For gross neural morphological assessments, brains were fixed in 4% paraformaldehyde, post-fixed for 4 h, and embedded in paraffin. Additional brain-sets were prepared for free-floating sections. For free-floating sections, brains were placed in 30% sucrose until fully saturated following post-fixation. Paraffin embedded brains was cut at 4 µm. Free-floating sections were cut at 30 µm. Paraffin sections were deparaffinised and boiled in sodium citrate buffer (2x5 min) for antigen retrieval. All sections were treated with 1% H_2O_2 for 10 min to quench endogenous peroxidase activity and blocked with 5% serum plus 1% BSA and 0.3% Triton X-100 for 30 min. Every 100 µm section was stained using NeuN (MAB377, Millipore) and parvalbumin (P3088, Sigma) antibodies. Colormetric stains (hemotoxylin/eosin and solochrome) were used to observe structure and myelination patterns. Primary antibodies were incubated overnight at 4°C followed by incubation with secondary biotinylated antibodies (Dako) for 1 h at room temperature. Following secondary antibody, sections were incubated with streptavidin-biotin complex (Vectastain) for 1 h before being developed with diaminobenzidine and mounted with Pertex (HistoLab).

Western molecular weight analyses (Figure 3g/Table 2)

Tissue collection. WT and Df(h22q11)/+ mice were culled by cervical dislocation, the brains were removed, and the PFC, DStr and hippocampus were dissected and immediately frozen on dry ice before being stored at -80˚C.

Lysate preparation. Tissue was lysed with 10x volume of RIPA buffer (150 mM NaCl, 1.0% IGEPAL® CA-630, 0.5% sodium deoxycholate, 0.1% SDS, 50 mM Tris, pH 8.0) containing phosphatase and protease inhibitors (Thermo Scientific). Each sample was sonicated 3 times for 10 s and then centrifuged for 10 min at 4˚C (>10,000g). Protein concentration was measured on an Emax precision microplate reader (Molecular Devices, Sunnyvale, CA, USA) using the Pierce BCA protein assay kit (Thermo Scientific).

Western molecular weight analyses. Simple Western molecular weight analyses were performed according to the ProteinSimple user manual. In brief, lysate samples were mixed with a master mix (ProteinSimple) to a final concentration of 1x sample buffer, 1x fluorescent molecular weight markers, and 40 mM dithiothreitol (DTT) and then either heated at 95˚C for 5 min or left at room temperature, depending on the optimised conditions for each primary antibody. The samples, blocking reagent, primary antibodies, HRP-conjugated secondary antibodies, chemiluminescent substrate, and separation and stacking matrices were dispensed to designated wells in a 384-well plate. After plate loading, the separation electrophoresis and immunodetection steps took place in the capillary system and were fully automated. Peggy–Simple Western analysis is carried out at room temperature, and instrument default settings were used except as specified below. Capillaries were first filled with separation matrix, followed by stacking matrix and approximately 40 nl of sample loading. During electrophoresis, proteins were separated on the basis of molecular weight through the stacking and separation matrices at 250V for 40-45 min and then immobilized on the capillary wall using proprietary, photoactivated capture chemistry. The matrices

were then washed out. Capillaries were next incubated with a blocking reagent for 15 min, and target proteins were immunoprobed with primary antibodies, followed by HRP-conjugated secondary antibodies. Primary antibodies used were PSD-95 (Cell Signalling Technology (CST) #2507), Synaptophysin (CST #5461), Synapsin 1 (CST #2312), Drebrin (Medical and Biological Laboratories #D029-3), Gephyrin (Millipore #5725), NeuN (Millipore #N78), GFAP (CST #670), GluR1 (Anaspec #51516), GluR2 (Millipore #10529), NR2A (Sigma-Aldrich #M264), NR2B (NeuroMab #75-101), VGluT1 (Synaptic systems #135303), GAD65/67 (Abcam #55412), $GABA_A$ α1 (Millipore #5592), KCC2 (Millipore #07-432) and VGAT (Synaptic Systems #131011). All primary antibodies were diluted in antibody diluent (ProteinSimple) with a 1:25, 1:50 or 1:800 dilutions. The antibody incubation time was 120 or 180 min. Luminol and peroxide (ProteinSimple) were then added to generate chemiluminescence, which was captured by a charge-coupled device (CCD) camera. The digital image was analysed with Compass software (ProteinSimple), and the quantified data of the detected proteins was reported for the HET mice as percentage of WT signal, normalised to the housekeeping gene Pan Cadherin. Pan Cadherin was used as the housekeeping gene as it showed no significant difference between the sample groups, and is a very robust marker to run on the Peggy system, with a mean coefficient of variation (CV) below 20. Any markers that showed significant percentage change between genotypes in the original study was initially repeated using a new sample and master mix dilution. For cost and time limitations, a second replication study was run where all markers were measured using pooled samples. Here, the same 11 WT and 11 HET samples were pooled separately and run on the Peggy machine against each marker twice.

Microdialysis (Figure 4)

Drugs and reagents. HPLC reagents were of analytical grade and obtained from Merck (Darmstadt, Germany). Veratridine and

phenciclidyne hydrochloride (PCP) were purchased from Sigma-Aldrich (Madrid, Spain) and nomifensine from Tocris (Madrid, Spain). Veratridine was dissolved in DMSO and nomifensine in artificial CSF (aCSF). Concentrated solutions (5 mM and 1 mM, respectively) were stored at -20°C and working solutions, diluted in aCSF at the stated concentrations, and prepared immediately before local application through the dialysis probe. PCP was dissolved in saline.

Microdialysis procedure. A detailed description of the probe manufacture and microdialysis procedure can be found elsewhere (5). Anesthetized mice (sodium pentobarbital, 30 mg/kg, i.p.) were stereotaxically implanted with concentric microdialysis probes equipped with a Cuprophan membrane (1.5 mm long) in the DStr at AP: +0.5, ML −1.7, DV −4.5 mm from Bregma and skull surface (1). Microdialysis was performed in freely moving mice >20 h after surgery. Probes were perfused with aCSF (125 mM NaCl, 2.5 mM KCl, 1.26 mM $CaCl_2$, 1.18 mM $MgCl_2$) and pumped at 1.5 µl/min. Dialysate fractions were collected every 20 min. After collection of baseline dialysate fractions, a local pulse (20 min) of the depolarizing agent veratridine (50 µM) was administered by reverse dialysis. Following recovery of basal values, the DA uptake inhibitor nomifensine (50 µM) was applied by reverse dialysis. On the following day, the same mice were used to examine the effect of systemic administration of PCP (2.5 + 2.5 mg/kg s.c.) on extracellular DA levels in the striatum. After a 60 min (veratridine and nomifensine) or 180 min (PCP-treated animals) stabilisation period, 4-5 fractions were collected to obtain basal values before local (reverse dialysis) or systemic drug administration. Thereafter, successive 20 min dialysate samples were collected. The concentration of DA in dialysate samples was determined by HPLC, using a modification of a previously described method (6). Brain dialysates were collected on micro vials containing 5 µl of 10 mM perchloric acid and were rapidly injected into the HPLC. DA was amperometrically

detected at 5–7.5 min with an absolute limit of detection of 2–3 fmol/sample using an oxidation potential of +0.75 V (Hewlett-Packard 1049 amperometric detector). Fractions 4-5 were used to determine the concentration of dopamine (DA), glutamate (Glu), homovanilic acid (HVA) and 3,4-dihidroxyphenylacetic acid (DOPAC) in basal conditions (5;7;8).

Supplementary results

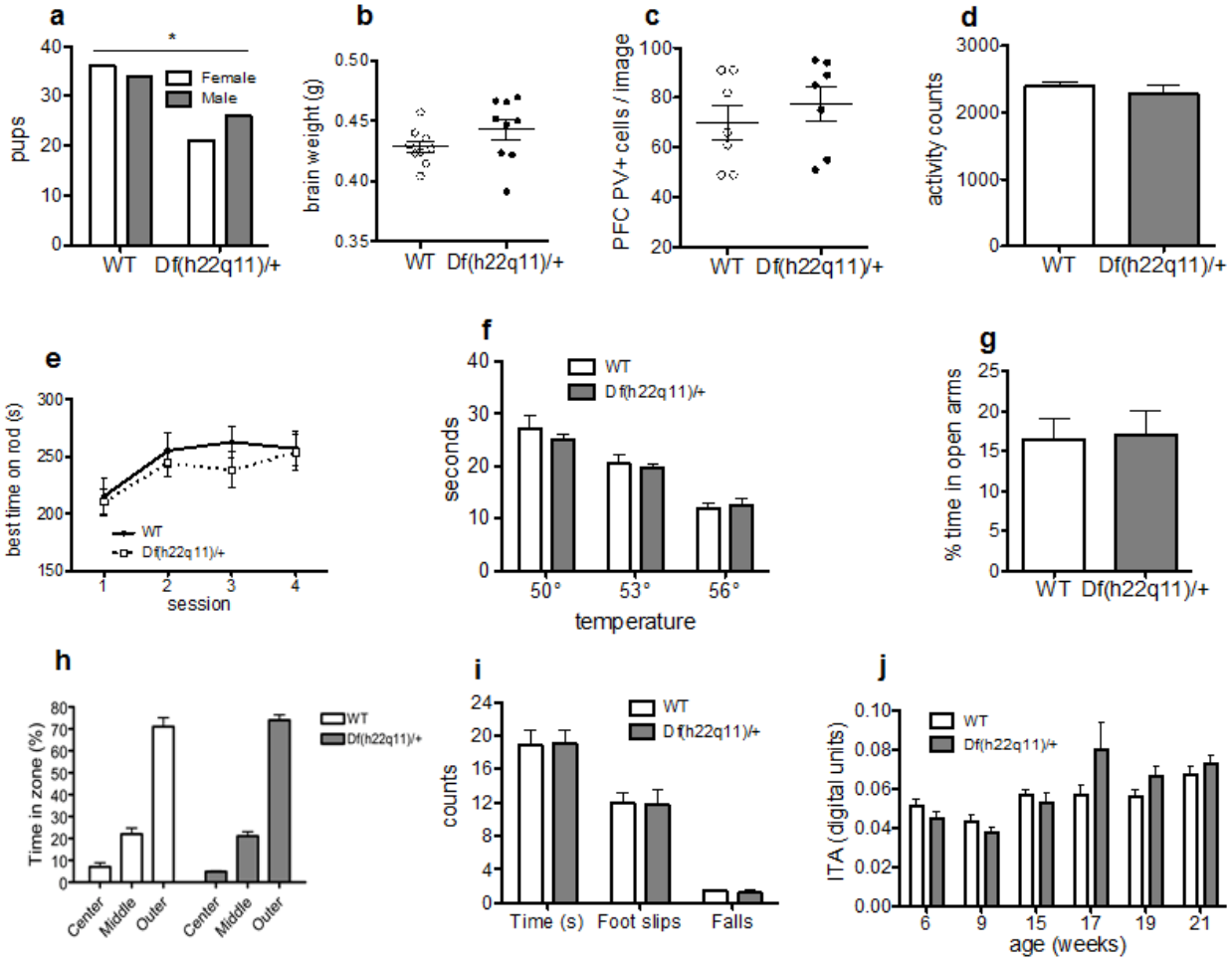

Supplementary Figure A3. Characterisations of Df(h22q11)/+ and WT littermates. (a) Birth ratios. The Df(h22q11)/+ mutant has decreased in utero survival (Total N = 117, WT N = 70, TG N = 47; p = 0.047, binomial distribution). (b) Brain weight. No effect of genotype ($F_{1,16} = 2.107$, $p = 0.166$). (c). PFC parvalbumin positive cells. No effect of genotype ($F_{1,12} = 0.650$, $p = 0.436$). (d) Basal locomotor activity. No effect of genotype on 60min open-field activity ($F_{1,93} = 0.618$, $p = 0.434$) (e). Rotarod. No effect of genotype (genotype: $F_{1,18} = 0.343$, $p = 0.565$; genotype × session $F_{3,54} = 1.058$, $p = 0.374$). (f) Hot plate test. No

effect of genotype ($F_{1,20} = 0.219$, $p = 0.645$) or genotype × temperature interaction ($F_{1,40} = 0.906$, $p = 0.412$). (g) Elevated plus maze. No effect of genotype on percent time in open arms ($F_{1,22} = 0.018$, $p = 0.894$). (h). Bright open field (120 lux). No effect of genotype ($F_{1,90} = 0.000212$, $p = 0.988$) or genotype × zone ($F_{2,90} = 0.557$, $p = 0.575$). (i) Beam-walking. No effect of genotype on time spent on beam ($F_{1,30} = 0.006$, $p = 0.938$) foot slips ($F_{1,30} = 0.008$, $p = 0.929$) or falls ($F_{1,30} = 0.338$, $p = 0.565$). (j) PPI inter-trial activity (ITA). No effect of genotype in 6 independent cohorts aged between 6-21 weeks ($p \geq 0.129$). Asterisk denote differences at which $p < 0.05$

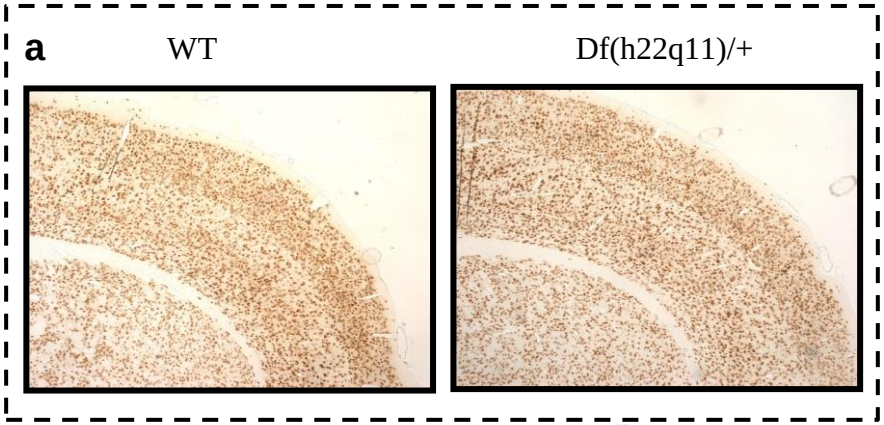

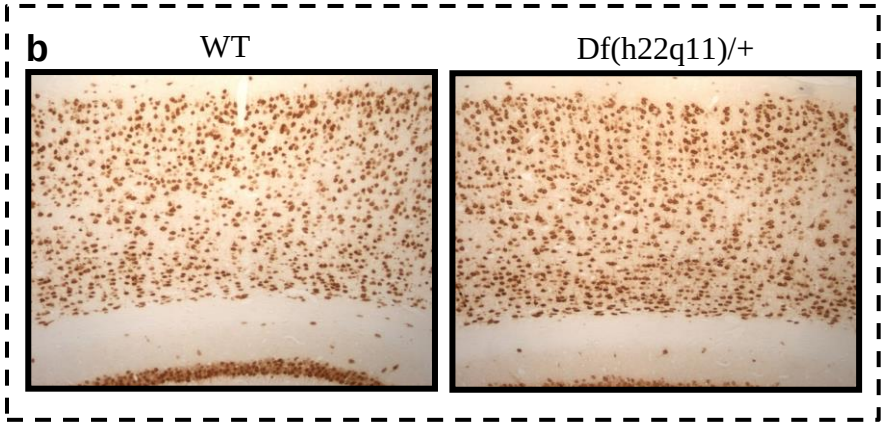

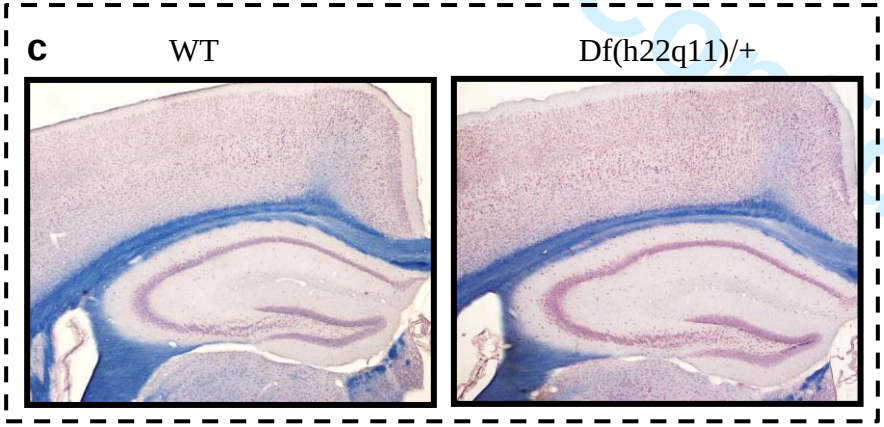

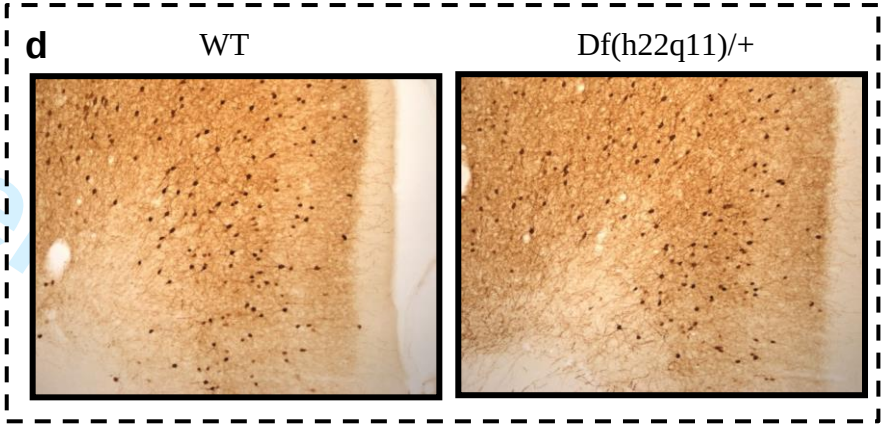

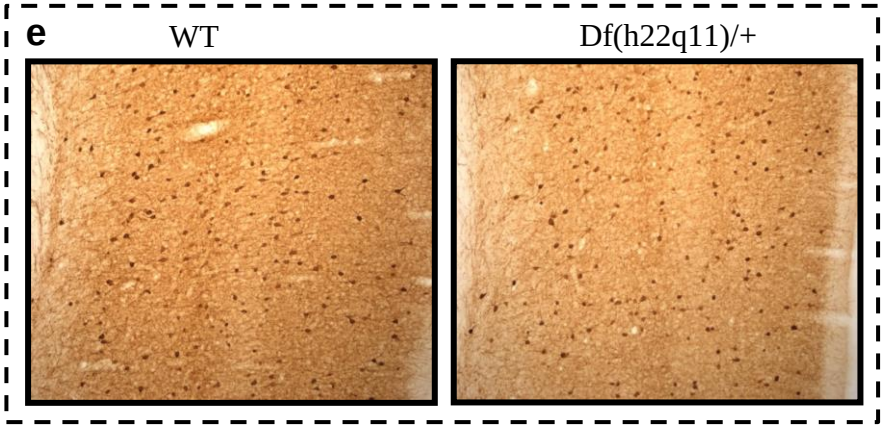

Supplementary Figure A4. Anatomical and histological evaluation of 10-week old WT (left panels) and Df(h22q11)/+ (right panels) littermates. **(a-b)** Cortical NeuN immunoreactivity. **(c)** Dorsal hippocampal solochrome stain. **(d)** Parvalbumin immunoreactivity in PFC. **(e).** Parvalbumin immunoreactivity in motor cortex.

Model	Df(h22q11)/+	Df(16)A+/-	LgDel	Df1/+	
Deletion	Dgcr2-Hira	Dgcr2-Hira	Dgcr2-Hira	Dgcr14-Ufd11	Znf74-Ctp
Strain	C57/Bl6N	C57/Bl6J	C57/Bl6N	Mixed C57/Bl6C-/C-; 129S5/SvEvBrd	129SvEvTac or mixed 129SvEvTac
Test Battery					
Body weight	x	x	x[9]	–	X[10]
Brain weight	x	–	x[9]	–	–
Beam walk	x	–	–	–	–
Rotarod	x	–	x[11]	x[12]	↓[10]
Locomotor activity	x	↑[13]	–	–	–
Thermal pain	x	–	↑[11]	x[12]	x[10]
Elevated plus maze	x	–	–	–	–
Bright open	x	–	–	–	–

field

Supplementary Table A1. Summary of results from basic charactarisations for the Df(h22q11)/+ mutant and other 22q11.2DS mouse models. ↓ decreased, ↑ increased, ╳ no effect, - no data.

Supplementary references

1. Paxinos G, Franklin KBJ. The Mouse Brain in Stereotaxic Coordinates. London: Elsevier Academic Press; 2008.242 p.

2. Debarbieux F, Brunton J, Charpak S. Effect of bicuculline on thalamic activity: a direct blockade of IAHP in reticularis neurons. J Neurophysiol. 1998 Jun;79(6):2911-8.

3. Steward O, Tomasulo R, Levy WB. Blockade of inhibition in a pathway with dual excitatory and inhibitory action unmasks a capability for LTP that is otherwise not expressed. Brain Res 1990 May 21;516(2):292-300.

4. Tepper JM, Martin LP, Anderson DR. GABAA receptor-mediated inhibition of rat substantia nigra dopaminergic neurons by pars reticulata projection neurons. J Neurosci 1995 Apr;15(4):3092-103.

5. Diaz-Mataix L, Scorza MC, Bortolozzi A, Toth M, Celada P, Artigas F. Involvement of 5-HT1A receptors in prefrontal cortex in the modulation of dopaminergic activity: role in atypical

antipsychotic action. J Neurosci 2005 Nov 23;25(47):10831-43.

6. Ferre S, Cortes R, Artigas F. Dopaminergic regulation of the serotonergic raphe-striatal pathway: microdialysis studies in freely moving rats. J Neurosci 1994 Aug;14(8):4839-46.

7. Adell A, Sarna GS, Hutson PH, Curzon G. An in vivo dialysis and behavioural study of the release of 5-HT by p-chloroamphetamine in reserpine-treated rats. Brit J Pharmacol 1989 Apr 30;97(1):206-12.

8. Lopez-Gil X, Babot Z, Amargos-Bosch M, Sunol C, Artigas F, Adell A. Clozapine and haloperidol differently suppress the MK-801-increased glutamatergic and serotonergic transmission in the medial prefrontal cortex of the rat. Neuropsychopharmacol. 2007 Oct;32(10):2087-97.

9. Meechan DW, Maynard TM, Tucker ES, LaMantia AS. Three phases of DiGeorge/22q11 deletion syndrome pathogenesis during brain development: patterning, proliferation, and mitochondrial functions of 22q11 genes. Int J Dev.Neurosci 2011 May;29(3):283-94.

10. Kimber WL, Hsieh P, Hirotsune S, Yuva-Paylor LA, Sutherland HF, Chen A, Ruiz-Lozano P, Hoogstraten-

Miller SL, Chien KR, Paylor R, et al. Deletion of 150 kb in the minimal DiGeorge/velocardiofacial syndrome critical region in mouse. Hum Mol Genet 1999 Nov 1;8(12):2229-37.

11. Long JM, LaPorte P, Merscher S, Funke B, Saint-Jore B, Puech A, Kucherlapati R, Morrow BE, Skoultchi AI, Wynshaw-Boris A. Behavior of mice with mutations in the conserved region deleted in velocardiofacial/DiGeorge syndrome. Neurogenetics 2006 Aug 10;7(4):247-57.

12. Paylor R, McIlwain KL, McAninch R, Nellis A, Yuva-Paylor LA, Baldini A, Lindsay EA. Mice deleted for the DiGeorge/velocardiofacial syndrome region show abnormal sensorimotor gating and learning and memory impairments. Hum Mol Genet 2001 Nov 1;10(23):2645-50.

13. Stark KL, Xu B, Bagchi A, Lai WS, Liu H, Hsu R, Wan X, Pavlidis P, Mills AA, Karayiorgou M, et al. Altered brain microRNA biogenesis contributes to phenotypic deficits in a 22q11-deletion mouse model. Nat Genet 2008 May 11;40(6):751-60.